Size Exclusion Chromatography of DNA and Viruses: Properties of Spherical and Asymmetric Molecules in Porous Networks

M. Potschka

Max Planck Institute for Biophysical Chemistry, Am Fassberg, D-3400 Goettingen, Federal Republic of Germany, and Porzellangasse 19, A-1090 Vienna, Austria

Received May 29, 1990; Revised Manuscript Received April 26, 1991

ABSTRACT: This article attempts a general theoretical description of size exclusion chromatography (SEC) derived from novel supportive experiments on some key issues as well as from critically reviewed data from the literature. The elution volume of SEC is stringently derived from thermodynamic principles as the volume accessible to the center of gravity of a solute within a porous matrix. It is thus related to the size of the solute. This size is defined energetically from the interaction energy between the solute and the matrix wall and thus entails a "hard core contour" of the solute plus interfacial interaction energies and entropic terms. Variation of the ionic strength of the aqueous solvent and comparison of solutes of widely different size and shape demonstrate that electrostatic forces alone are insufficient to explain the experimental results. Instead, retarded van der Waals forces are crucial. Below some 3 nm, hydration forces dominate, and interfacial separation becomes independent of electrostatic forces. Due to the observed huge size dependency of interfacial separation, porous networks, established by these phenomena, are nonetheless permeable to smaller macromolecules, which is crucial for biology. Given the proper description of interfacial separation for a particular mutual orientation between the matrix wall and an arbitrary shaped solute, the average overall configurations, i.e., a proper rotational average of the solute molecule, must be taken. It appears that a hydrodynamic equivalent radius based on intrinsic viscosity is best suited to define the rotational averaging of the hard core contour. The remaining discrepancies, probably related to insufficient definition of some systems and their nonchromatographic reference data, remain to be settled, however. The quest for universal calibration of SEC has thus been generalized into a comprehensive physicochemical description of permeated porous materials.

Introduction

Size exclusion chromatography (SEC) (Table I) is both an important tool for the characterization of macromolecules and an intriguing model system for supramolecular organization. The theoretical premises of the method are, furthermore, all but resolved. In this regard, two principal issues are of concern at present. The first quest is finding out whether a universal size parameter exists that characterizes the elution of macromolecules of all shapes. The second quest is the search for a framework that accounts for the charge interactions and other interfacial phenomena between the matrix and a polyelectrolyte solute.

I have previously reported[1,2] that the chromatographic size of a solute may be described as being additively composed of two terms. The first term is the viscosity radius as determined hydrodynamically in bulk solution. The second term reflects the charge repulsion between the matrix wall and the macromolecule and is scaled by $I^{-1/2}$. At high ionic strength, the second term may be neglected, and it is possible to deal with the first issue of particle shape separately. I have reported that all classes of macromolecules, regardless of their shape being solid spheres, expanded coils, or more or less flexible rods, elute according to a universal size parameter (Table I), namely, the viscosity radius, R_η, which is equivalent to the hydrodynamic volume, $[\eta]M$. Significant discrepancies occurred upon attempting to use the diffusional Stokes radius, R_S, radius of gyration, R_G, or mean linear extension instead. In particular, these observations were found to apply to DNA when compared to proteins and viruses of various shapes. Small variations were attributed to residual charge effects or inaccurate hydrodynamic literature data. Recently, Dubin and Principi[3] reported on the failure of this concept by demonstrating that schizophyllan and DNA elute earlier than predicted by R_η, albeit much later than according to R_G. The authors suggest that discrepancies may be related to the stiffness of the rod and that they become more pronounced for rods shorter than their persistance length. This view acknowledges the fact that flexible rods of increasing length gradually form coils and coils were shown to elute according to R_η. The assertion that DNA violates the principles of universal calibration is entirely dependent on a proper choice of Mark–Houwink coefficients relating molecular weight to intrinsic viscosities.

In the present report, the elution of DNA and viruses on SEC columns is examined in more detail, aimed at resolving the issue of interfacial phenomena. Thus, previous data concerning charge effects[2] are extended and notions on this subject elaborated on. In its main part, a general theoretical analysis of SEC is provided. The entropy of the system is now explicitly incorporated into the model. Interfacial contributions are explained by the DLVO theory of colloidal stability[4] but not by electrostatic repulsion alone. The retardation of van der Waals forces is found to be crucial. Concerning the issue of hydrodynamic shape, the chromatographic experiments of Dubin and Principi[3] with regard to DNA are validated, but conflicting evidence with respect to their interpretation is provided.

Analysis of the SEC elution volume is split into a term, R_{SEC}, related to properties also found in bulk solution and a second term, R_{IF}, due to interfacial effects. Only by appreciating the charge-related effects as a special case of interfacial interaction is it possible to grasp the nature of the universal calibration. The analyses of R_{SEC} on the one hand and R_{IF} on the other thus are inseparable facts of the general theory of SEC. This paper is arranged as follows:

The Results section (1) presents experiments with DNA analyzed in a manner that presumes to cancel interfacial effects, which are principally present at all times in a packed column. Next, interfacial effects are singled out

0024-9297/91/2224-5023$02.50/0

Table I
Abbreviations Used[a]

SEC	size exclusion chromatography
IEC	ion-exchange chromatography
HIC	hydrophobic interaction chromatography
DLVO	Dejaguin–Landau–Verwey–Overbeek (theory of colloidal stability)
CPG	controlled porous glass
GuHCl	guanidine hydrochloride
SDS	sodium dodecyl sulfate
PAGE	poly(acrylamide) gel electrophoresis
PEG	poly(ethylene glycol)
PSS	poly(styrene sulfonate)
PAA	poly(acrylic acid)
PEI	poly(ethylenimine)
PVA	poly(vinylamine)
PVAc	poly(*N*-vinylacetamide)
PVA1	poly(vinyl alcohol)
PVP2	poly(2-vinylpyridine)
PVP4	poly(4-vinylpyridine)
PVPn	poly(*N*-vinylpyrrolidone)
PDMDAAC	poly(dimethyldiallylammonium chloride)
PLys	poly(lysine)
PGlu	poly(glutamic acid)
TBSV	tomato bushy stunt virus
TYMV	turnip yellow mosaic virus
Qβ	bacteriophage Qβ
MS2	bacteriophage MS2
*Hae*II, *Hin*dIII, *Eco*RI, *Eco*RV, *Ssp*I, *Sca*I, *Pst*I	various restriction enzymes
pJW200, pBR222	various DNA plasmids
Definition of Radii	
R	total solute radius strictly defined in eq 34
R_{IF}	interfacial contribution to R (eq 34)
R_{SEC}	chromatographic equivalent radius of the body (rotational average body size) (eq 34)
R_S	equivalent body radius defined by diffusion (Stokes radius)
R_η	equivalent body radius defined by intrinsic viscosity (eq 2)
R_G	equivalent body radius defined by X-ray or light scattering (radius of gyration)

[a] R_S, R_η, R_{SEC}, and R_G all differ by giving different weights to the asymmetry of the body. Identifying the properties of R_{SEC} is one-half of the issues of this paper. $R_{IF} = 2[((c(mg/mL)v)/1000\xi)^{-1/3} - 1]R_S$, with a typical packing density of $\xi \sim 2/3$ for spheres of equal size and a partial specific volume of $v = 0.73$. Note that according to Figure 6 $R_{IF} \propto R_S^{1/2}$; i.e., aggregate formation increases solubility.

by varying the ionic strength. It is first shown (2) that this has a negligible effect on the mechanic structure of the matrix. Next, a phenomenological equation suitable for data reduction to a few key terms is presented (3). Lastly (4), the Results section mathematically describes the physics of the interfacial phenomena taking place during the process of SEC.

The Discussion section initially presents published data from the literature split according to topical issues. It follows the same separation on noninterfacial effects, discussed first (1–4), and interfacial effects, discussed second (5). After the start with a general overview on universal calibration (1) follows a section on DNA excluding interfacial effects (2), the role of lipids and surfactants (3), and open issues in universal calibration (4). Section 6 concludes with some biological corollaries followed by a brief summary.

Experimental Section

1. Size Exclusion Chromatography. The chromatographic instrumentation has been described in detail previously.[1,2] The data reported were obtained with two different TSK 6000 PW (TosoHaas/Pharmacia) 60-cm stainless steel columns operated at a flow rate of 10 mL/h. One of them was used previously,[2] and both gave identical results also with respect to ionic strength dependency. DNA elution was monitored at 260-nm absorbancy, viruses mostly at 280 nm. Injection volumes were 10 μL for analytical runs and up to 200 μL preparatively. The analytical conditions were experimentally verified to pertain to conditions of infinite dilution. Basically this requires that the ionic strength contribution of the solute is negligible, which sets a practical lower limit of 2 mM ionic strength for the eluent. Agarose gel electrophoresis of DNA after SEC measurements assured that shear degradation was absent. Supplementary data have also been gathered on a TSK 5000 PW-2, a column previously used,[2] that appears to bear more surface charges than the TSK 6000 PW columns used here.

2. Materials. The samples used for calibration were as described previously.[1,2] TBSV and TYMV were kindly provided by J. Witz, Strassbourg; Qβ and MS2 were a gift from C. Biebricher, Goettingen. Human erythrocyte spectrin was provided by S. Eber, Goettingen, and the hemolymph of *Eurypelma californicum* from H. J. Schneider, Munich, was used to study hemocyanin. TMV was prepared as described previously.[5] The starting material for the linear double-stranded DNA restriction fragments was pJW200, a shortened pBR222 plasmid.[6] In addition a 195 (±40) bp (base pair) mixture of calf thymus DNA, which was the same batch studied previously[1] and was provided by C. Kleinschmidt, Goettingen, was used. Restriction enzymes were from New England Biolabs.

3. Preparation of DNA. pJW200 is a deletion construction obtained from pBR322 by deleting parts of the Tet^{res} gene between two *Hae*II sites at positions 232 and 2349 of pBR322.[6] pJW200 (2246 bp) was transformed into *E. coli* HB101 cells. The transformed cells were grown to saturation; the alkaline plasmid was extracted and purified by HPLC on a Nucleogen 4000 column (Diagen). The obtained pJW200 was fragmented first with *Hind*-III followed by *Eco*RI (New England Biolabs, buffers as suggested by the manufacturers) to obtain a short (29-bp) and a long (2217-bp) linear DNA fragment. The complete cutting of the plasmid by the two enzymes was checked on a 0.7% agarose gel. The fragments were separated on the HPLC Nucleogen 4000 column applying a salt gradient as suggested by the manufacturer. The separated fragments were dialyzed, and ethanol was precipitated. No impurities could be detected on the HPLC diagram or by agarose gel electrophoresis.

From the longer DNA fragment (2217 bp), single cut cleavage fragments were prepared by digestion with the restriction enzymes (New England Biolabs) *Eco*RV (yielding fragments with length 156 and 2061 bp), *Ssp*I (193, 2024 bp), *Sca*I (517, 1700 bp), or *Pst*I (754, 1463 bp). *Eco*RV, *Ssp*I, and *Sca*I cut with blunt ends; the other restriction enzymes produce a 4-bp single-stranded sticky end. Thus, all DNA pieces have one sticky side (i.e., are 2 bp longer); those cut by *Pst*I and the 2217-bp fragment itself have two sticky sides. Again, the complete cutting of the fragment by the enzymes was checked on 0.7% agarose gels. Fragments were separated and enzymes removed by SEC in the buffers used for subsequent analysis. Alternatively, the fragments were separated on the HPLC Nucleogen 4000 column applying a salt gradient. The separated fragments were dialyzed, and ethanol was precipitated. The HPLC diagram showed no impurities. On a poly(acrylamide) gel (8%), some short fragments displayed additional small contaminating bands that, however, never exceeded 3% of the total amount of DNA. No longer contaminant bands were seen by agarose gel electrophoresis. Besides the characteristic short single-stranded tails, all DNA was in linear double-stranded conformation and contained no unusual sequences.

Results

1. Determination of Chromatographic Viscosity Radii for DNA. Elution volumes of linear double-stranded DNA were compared with those of reference

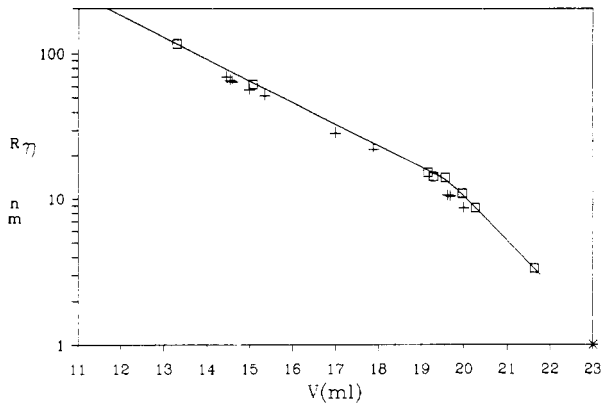

Figure 1. TSK 6000 PW column calibrated with spherical and rod-shaped viruses as well as globular proteins according to their viscosity radii. The reference samples are TMV dimer, TMV, TYMV, Spectrin dimer, MS2, hemocyanin, thyroglobulin, alkaline phosphatase (□). V_{tot} was measured with vitamin B_{12} (*). At the same time, linear double-stranded DNA restriction fragments were chromatographed (+). They elute earlier than predicted by their intrinsic viscosity according to eq 1. Eluent: 8 mM sodium phosphate, 1 mM sodium salt of EDTA, pH 6.85, and 179 mM sodium chloride (total I = 200 mM).

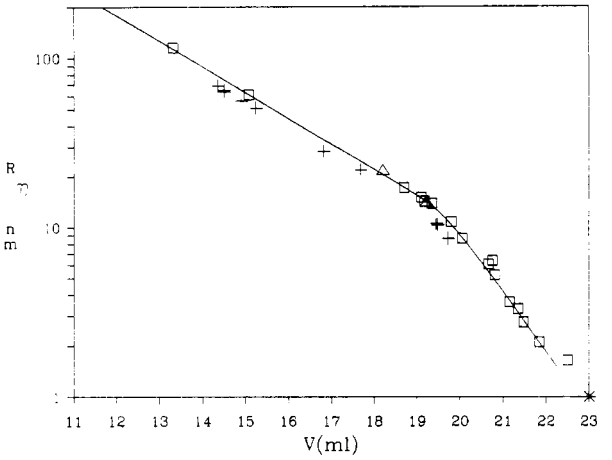

Figure 2. Same column shown in Figure 1 calibrated at a lower ionic strength. The reference samples are TMV dimer, TMV, TBSV, TYMV, Qβ, MS2, hemocyanin, thyroglobulin, urease, apoferritin, catalase, BSA, alkaline phosphatase, ovomucoid, carbonic anhydrase, cytochrome c (□); spectrin tetramers and dimers (△); V_{tot} (vitamin B_{12}) (*); DNA restriction fragments (+). Eluent: 8 mM sodium phosphate, 1 mM sodium salt of EDTA, pH 6.85, and 37 mM sodium chloride (total I = 60 mM).

compounds, largely spherical viruses for smaller sized DNA and TMV, a rod-shaped stiff virus, and its axial dimer for large DNA fragments (Figure 1). For DNA at high ionic strength ($I \sim$ 50–200 mM), the Mark–Houwink coefficients determined by Eigner and Doty[7] with ultrasonically fragmented DNA were used

$$[\eta] = 1.05 \times 10^{-5} M_{\eta s}^{1.32} \quad (1)$$

where the units of $[\eta]$ are mL g^{-1} and molecular mass is in daltons. The same equation was used by Dubin and Principi.[3] Viscosity radii are operationally defined by intrinsic viscosity as follows

$$R_\eta \text{ (nm)} = \frac{3 \times 10^{24}}{10\pi N_L}([\eta]M)^{1/3} = 0.0541([\eta]M)^{1/3} \quad (2)$$

which simply converts a molar volume into a particle-equivalent radius. Thus, for solid spheres, $R_\eta = R_S$. Figure 1 demonstrates that on the basis of eq 1 all sizes of DNA elute slightly but consistently earlier than proteins and viruses. To exclude that this was due to a residual charge effect, measurements were repeated at lower ionic strength. Figure 2 shows that the difference between DNA and other samples does not increase. A more comprehensive study of ionic strength dependency reported below demonstrates that the extent of the charge effect is the same for DNA and viruses of similar size and thus confirms in detail that charge effects are ruled out as an explanation of premature DNA elution. Note that calibration lines at different ionic strength are different; a direct comparison is shown in Figure 5 of ref 2. Note further that the upper end of the calibration is entirely based on TMV and its dimer, which are rods substantially stiffer than DNA (see Discussion section). Thus, DNA and TMV of similar R_η should at least coelute even if their chromatographic radii were larger than R_η. The observations of Dubin and Principi[3] even predict that DNA should elute later in comparison. Premature elution of DNA thus does not converge to the normal elution of coils as DNA size increases. It does not seem to be related to persistence length and appears to be independent of double-layer size effects.

A more comprehensive view of DNA elution is obtained if one considers the calibration line obtained from the proteins and virus as the true universal calibration and converts DNA elution values into R_{SEC} radii on the basis of this calibration. One then finds virtually identical R_{SEC} values for small-sized DNA fragments regardless of ionic strength. Larger DNA, on the other hand, is somewhat more expanded at lower ionic strength, as one might have guessed (see Discussion section). For the sake of comparison, a distribution of restriction fragments studied previously[1] was redetermined. This sample was characterized by gel electrophoresis as having an average size of 195 bp. It eluted minutely ahead of the monodisperse restriction fragment from pJW200 containing 193 bp (see Figures 1 and 2).

Since linear DNA represents a homologous series of polymers, one may establish a relationship between these chromatographic radii and DNA size. Figure 3 presents such a correlation for the data at I = 60 mM ionic strength. One obtains

$$R_{SEC} \text{ (nm)} = 0.23(\text{bp})^{0.76} \quad (3)$$

with a correlation coefficient of r = 0.9995. Using eq 2, one may convert eq 3 into a Mark–Houwink equation (using an average molecular weight of 660 per base pair). At I = 60 mM, one obtains

$$[\eta]_{SEC} = 2.4 \times 10^{-5} M^{1.29} \quad (4)$$

Similarly, one may analyze the data at I = 200 mM and find

$$R_{SEC} = 0.24(\text{bp})^{0.75} \quad (5)$$

$$[\eta]_{SEC} = 3.7 \times 10^{-5} M^{1.25} \quad (6)$$

The same exponent was found by Godfrey and Eisenberg,[8,9] who reevaluated the intrinsic viscosities of similar sized sonicated calf thymus DNA at a well-defined I = 200 mM, but their coefficient is only 2.3 × 10^{-5}, which essentially confirms the earlier data. The different exponents (eqs 4 and 6) may reflect the differing electrostatic coil expansion at different ionic strength. The effects are, however, very minor at these ionic strengths and currently will be ignored in the further analysis. The $[\eta]_{SEC}$ values are approximately 40–60% larger than the values of Godfrey[8] and Eigner and Doty[7] based on sonicated DNA. Equation 1 has been calculated from $M_{\eta s}$

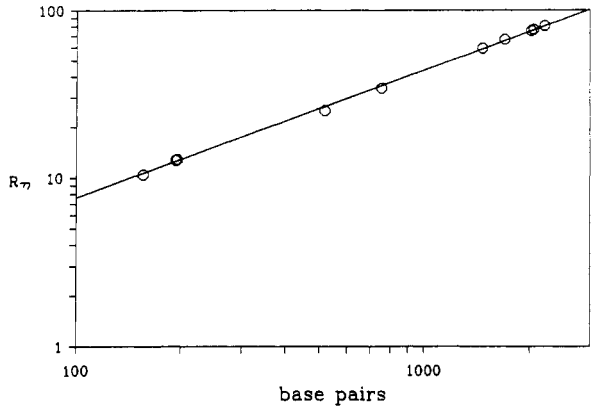

Figure 3. Relationship between chromatographic radii and molecular weight expressed in bp. DNA elution volumes from Figure 2 were matched to the calibration line obtained from the non-DNA reference compounds and the R_{SEC} values for the DNA restriction fragments deduced from this graph not from their intrinsic viscosities according to eq 1.

values, which in the case of DNA are smaller than M_η as follows:

$$M_\eta = \left(\frac{\sum c_i M_i^b}{\sum c_i}\right)^{1/b} \simeq M_w\left(\frac{M_w}{M_n}\right)^{(b-1)/2} \quad (7)$$

where the right-hand approximation is exact for a Lansing–Kraemer[10] log-normal distribution with $M_w/M_n = M_z/M_w$ and b is the Mark–Houwink exponent. Sedimentation coefficients were measured with the scanner and thus are weight averages rather than z averages such that the Scheraga–Mandelkern equation (which the authors used) reads

$$M_{\eta S} = (\text{constant})s^{3/2}[\eta]^{1/2}\left(\frac{R_\eta}{R_S}\right)^{-3/2} \simeq M_w\left(\frac{M_w}{M_n}\right)^{(3/4)[(d^2-d)(1-2\epsilon)+[(b^2-b)/3]]} \quad (8)$$

where $R_\eta/R_S = (\text{constant})M^\epsilon$ ($\epsilon = (b + 1)/3 - d$); $R_S = (\text{constant})\ M^d$ is a measure of asymmetry. Thus, eq 1 is biased by the largely unknown size distribution of these DNA samples but the difference between eqs 7 and 8 is small enough for DNA that errors are likely below 10% and, in any case, in opposite direction to the present discrepancy. The assumption of Eigner and Doty that follows seems more critical. They assume that $\epsilon = 0$, given that for DNA $\epsilon \sim 0.02$–0.04, which easely could yield errors of a factor of 2 in the right direction. Combined viscosimetry and light-scattering data,[9] however, suggest that the empirically chosen constant Scheraga–Mandelkern parameter reasonably cancelled all errors. Lastly, however, it is conceivable that DNA which is fragmented by sonication also contains single-strand breaks, which reduces stiffness, and thus, a lower intrinsic viscosity would have been observed. $[\eta]$ values of restriction fragments or other DNA securely lacking strand breaks thus far have not been reported. Restriction fragments, demonstrated to lack nicks, sediment akin to sonicated or DNase degraded DNA.[11] This, however, does not preclude that intrinsic viscosities nonetheless differ since $[\eta]$ is more sensitive to flexibility than Stokes radii.[1] Thus, two reports on hydrodynamics diverging from the consensus remain to be mentioned: Interpolated to a 2217-bp DNA, Godfrey's s value is 8% larger than the above consensus,[7,11-13] while the intrinsic viscosity expressed as a viscosity radius is 12% smaller.[8] This evidence from two independent measurements makes plain error unlikely and is rather

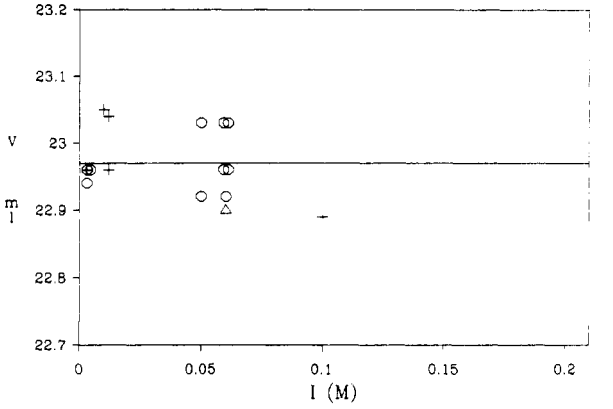

Figure 4. Retention volume of vitamin B_{12} in different aqueous buffers on a TSK 6000 PW column. Eluents: sodium phosphate + NaCl at pH 6.8 (Δ); Tris–HCl + NaCl at pH 8.0 (+); borate + NaF at pH 8.0 (○). Mean $V_{TOT} = 22.97 \pm 0.05$ mL including the dead volume of the chromatographic equipment.

Table II
Elution of TMV on TSK 5000 PW

I, mM	eluent	TMV	R, nm[a]	V, mL
4	borate/NaF, pH 8.2	monomer	>100[b]	10.28
214	sodium phosphate, pH 7.2	dimer	~123[c]	10.23
214	sodium phosphate, pH 7.2	monomer	~68[b]	10.41

[a] $R = R_\eta + R_H$. Interfacial separation was estimated from data on TSK 6000 PW (Figure 6). Applicable true values are likely to be somewhat larger, particularly at low ionic strength, since the TSK 5000 PW2 column seems to be more negatively charged. [b] $R_\eta = 61$ nm. [c] $R_\eta = 115$ nm.

well explained in terms of a more contracted DNA conformation. Similarly, my previously published s value for the 2217-bp molecule is 10% smaller than the consensus and thus would explain the 10% increase in R_{SEC}. However, intrinsic viscosities had not been directly measured. The circumstances of these observations remain to be revealed. The fact that premature elution was also observed for all further fragments derived from this 2217-bp molecule certainly excludes the presence of a localized unusual sequence responsible for increased stiffness. The fact is that premature elution was found to be unique for DNA and was not consistent with the notion that increasing stiffness increases deviation (as contradicted by the elution of TMV discussed above). Since any conclusion concerning the mechanism of SEC hinges on the proper choice of intrinsic viscosities, it seems necessary to first redetermine them by a conventional technique. Since this is a major task, it unfortunately goes beyond the means and scope of the current report.

2. Ionic Strength Dependency of the TSK PW Matrix Structure. To ascertain that the matrix itself does not mechanically change with changing ionic strength of the eluent, elution volumes of vitamin B_{12}, a practically totally included small neutral molecule, were measured (Figure 4). This demonstrates that V_{TOT} is virtually independent of the studied solvent conditions. The second criterion for a mechanically rigid matrix is a constant void volume, i.e., an unchanged pore size. Since suitable compounds were not immediately available, this was tested with the same material but a different pore size, TSK 5000 PW. Our elution volumes on this column[1] agree with those of Himmel and Squire,[14] whose erroneous analysis, however, suggested an entirely wrong void volume. The reciprocal of the maximum selectivity of this column is $d \ln R_\eta\ (\text{nm}) = -0.31\ dV\ (\text{mL})$. Table II, which lists the elution of TMV monomers and dimers at low and high

ionic strengths, demonstrates that the slope of the calibration around V = 10.3 mL is more than 10 times larger, -3.52, which identifies this region as the void volume. At high ionic strength, TMV monomers are barely included, and they become excluded at lower ionic strength because their effective size increases (see below). Table II thus demonstrates that $V_{VOID} \simeq 10.25$ mL is essentially independent of ionic strength. Insisting that the proper chromatographic radius does not increase with decreasing ionic strength, the void volume would shift by 0.1 mL, which is still negligible to the separation range of 11 mL of included volume. However, this assumption subsequently cannot explain the large shift, several milliliters, observed for well-included polyelectrolytes.[2] Thus, the TSK PW porous network is rigid and any changes of elution due to varying solvent conditions must be attributed to interfacial contributions and possibly to changing solute boundaries, i.e., varying R_η.

3. Ionic Strength Dependency of SEC Elution. Polyelectrolytes of whatever nature elute differently depending on ionic strength. This is exemplified in the different calibrations obtained for different ionic strengths shown in Figures 1 and 2. In the following, a more rigorous treatment of this charge effect following the reasoning outlined previously[2] will be reported. To this end, I briefly summarize the logic of my analysis: Two substances coelute from a column if they sample the same volume, no matter whether some portion of the total pore volume is unavailable to them due to steric exclusion or due to electrostatic repulsion. To measure the repulsion distance, one simply must know the size of a coeluting species devoid of electrostatic repulsion. The electrostatic repulsion is an interfacial effect not present in bulk solution (at infinite dilution) and therefore not measured by a conventional hydrodynamic technique. Thus, one first of all needs to establish an absolute calibration of chromatographic elution. Neutral macromolecules may serve this purpose. More conveniently, charge interactions become screened at sufficiently high ionic strength such that wall effects cease and viscosity radii determined in bulk solution may serve as absolute calibration. Note that a relative calibration is always possible as long as the macromolecules are similarly charged (see Figure 2). Having established such an absolute size scale for a given column, one may convert all elution volumes regardless of ionic strength to this absolute size. In practical terms, a polyelectrolyte at low ionic strength elutes earlier than predicted on the basis of bulk R_η values. Our procedure assigns a size equal to that of a neutral molecule that samples the same volume albeit for other reasons. Clearly, electrostatic repulsion is a matter of both the pore wall and the macromolecular solute. R is a measure of this distance of closest approach and not an exclusive attribute of the solute. The forementioned procedure is simply designed to eliminate column-specific aspects such as pore geometry and pore size distribution from subsequent analysis.

Having converted all of our primary data, only a fraction of which are shown in Figures 1 and 2, according to this description one may analyze these chromatographic radii as a function of ionic strength (Figure 5). Confirming previous data on this subject[2,15] and extending them to larger solute sizes, Figure 5 demonstrates that elution radii increase linearly with $I^{-1/2}$. For aqueous solutions at room temperature, one may therefore write

$$R = R_{SEC} + \kappa^{-1}\tilde{x} = R_{SEC} + 0.3I^{-1/2}\tilde{x} \qquad (9)$$

where $\tilde{x}$ is the average electrostatic repulsion distance at equilibrium in multiples of Debye length, and the units

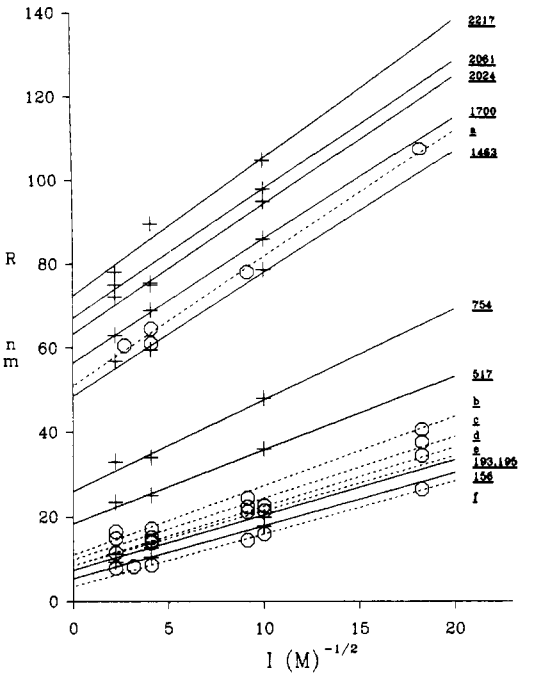

Figure 5. Ionic strength dependency of the elution of rod-shaped viruses (TMV (a)), spherical viruses (TBSV (b), TYMV (c), Qβ (d), MS2 (e)), globular proteins (thyroglobulin (f)) (○) and extended coils of DNA (sizes shown in bp) (+) in a variety of buffers between pH 6.85 and 8.00, e.g., DNA also in 8.1 mM Tris–HCl, 1 mM sodium salt of EDTA, pH 8.00 (total I = 10 mM). Elution volumes were converted into chromatographic radii via universal calibration at I = 200 mM (Figure 1) as described in the text. These radii are shown as a function of $I^{-1/2}$.

are nanometers for R and moles for I. $R_{SEC} = R_\eta$ for most substances but may be different for DNA and some other classes of elongated materials. Note that R_η sometimes is itself a complicated function of I. For the proteins and viruses studied previously[2] and here in Figure 5, R_η is effectively constant. For DNA, R_η presumably varies a little but the ionic strength dependency of small-sized DNA is unknown and therefore will be ignored initially (see Discussion section). From eq 9, one obtains

$$\tilde{x} = 3.3\, dR/dI^{-1/2} \qquad (10)$$

Note that $\tilde{x}$ is a universal parameter as it no longer depends on ionic strength but only on matrix charge and the size and charge of the solute polyelectrolyte.

4. Analysis of the Electrostatic Repulsion Distance. We have previously shown that above a certain threshold, an increase in net charge hardly increases the repulsion distance $\tilde{x}$ (in units of Debye length) for solutes of equal bulk size.[2] Knowing the charge densities of the samples studied in Figure 5, we are safely in this regimen. The matrix charge is a constant for the whole data set. One may thus analyze the dependency of the repulsion distance as a function of the geometric conditions only. Figure 6 presents repulsion distances, $\tilde{x}$, obtained from eq 9 without further corrections, as a function of R_{SEC}. It is seen that $\tilde{x}$ greatly increases with solute size. Note that linear DNA and spherical viruses of equal chromatographic radius, R_{SEC}, exhibit the same repulsion distances. This is not a trivial observation since the geometric setup for the electrostatic interactions is quite different. Note further that all distances are exceedingly large, which suggests that theoretical treatments will suffice to consider linearized potentials, thereby reducing the mathematical challenge appreciably.

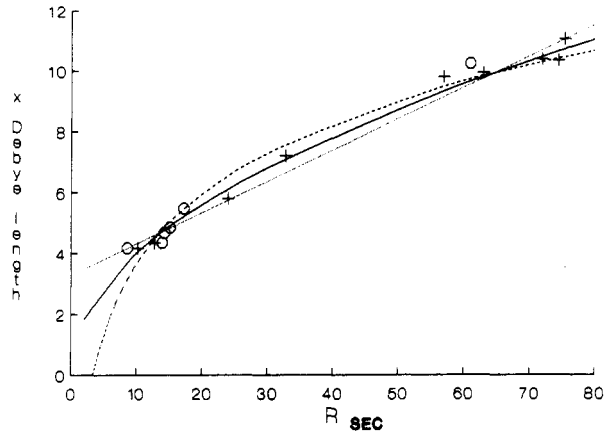

Figure 6. Size of the double layers repelling the macromolecule from the pore wall measured from the slope of the plots in Figure 5. They are shown as a function of the chromatographic radius of the core particle, i.e., R_{SEC}, measured at high ionic strength where the size of the diffuse double layer may be neglected as a first approximation. Proteins and viruses (O), DNA (+); power fit (exp = 0.486, regression coefficient r = 0.9916) (—), semilogarithmic fit (slope = 3.4, see Table III) (- - -), linear fit (r = 0.9897) (···).

Having demonstrated that chromatographic elution is not determined alone by hydrodynamic particle dimensions of bulk solution but also by interfacial effects between the matrix and solutes, it is obvious that the volume accessible to the solute is generally determined by the interaction energy between the matrix and solute

$$V(x) = V_e(x) + V_w(x) + V_s(x) + V_u(x) + V_o(x) \quad (11)$$

where e stands for electrostatic, w for van der Waals, s for solvation, u for undulation, and o for orientational energies. SEC is an entropic process, i.e., each solute molecule attempts to access the largest possible volume. This volume is obviously the volume accessible to the center of gravity of the solute molecule within the pores. In the traditional view, pore wall and solute are considered hard core bodies, which implies rectangular potentials. Acknowledging interfacial effects means acknowledging that all particle interactions are soft, defined by eq 11. The free-energy minimum of the entire system

$$\frac{dV}{dx} - T\frac{dS}{dx} = 0 \quad (12)$$

thus defines the closest approach between solute surface and containing wall where

$$S = k \ln\left(\frac{x_r - x}{x_r}\right)^n \quad (13)$$

with n being related to the fractal dimension. For an infinite system, $x_r \to \infty$, the entropic term vanishes. For a purely repulsive potential, surfaces are then pulled infinitely apart. For a pair interaction, n = 1; for a cylindrical containment, n = 2. For a general porous matrix, n depends on the surface-to-volume ratio and geometric parameters and is a noninteger constant characteristic of a particular porous matrix; typically n = 1.5 (up to 2.0) (reviewed in ref 2).

We will first analyze our observations exclusively in terms of electrostatic forces starting by considering the interaction between a sphere and a plane (Figure 7). The potential at a large distance from a planar surface is given by[4]

$$\psi = \psi_{S1} e^{-x} \quad (14)$$

where ψ_S is the saturation potential of the outer (linear) diffuse double layer and x is the distance between the two surfaces in units of Debye length. For a sphere of finite radius $A = \kappa R_\eta$, one obtains[4]

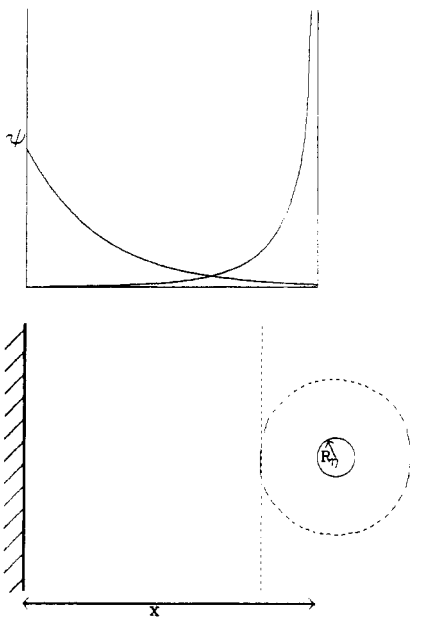

Figure 7. Schematic representation of the electrostatic repulsion between a sphere (to the right) and a plane (to the left). The plane is assumed to have a surface charge half the saturation level of the outer diffuse double layer. The double layer of the sphere is saturated, and counterion condensation is assumed on the surface. For detailed description, see text.

$$\psi = \psi_{S2}\frac{A}{x + A}e^{-x} \quad (15)$$

which decreases more rapidly for a small sphere as compared to a plane. This is illustrated in Figure 7 even under our assumption that $\psi_{S2} = 2\psi_{S1}$. The actual separation is determined by the interaction energy

$$V_e(x) = 4\pi\psi_{S1}\psi_{S2} f(R_\eta, x) e^{-x} \quad (16)$$

where V_e is in units of kT. $f(R_\eta)$ depends on the geometries involved, and ψ_S is a function of both surface charge and curvature of the surface. Ohshima et al.[16] calculated a very good approximation for the shape dependency of ψ_S. For maximally charged particles, their equation reduces to

$$\psi_S^{max} = \frac{8}{1 + \left(1 - \frac{2A + 1}{(A + 1)^2}\right)^{1/2}} \quad (17)$$

where ψ is in units of kT/e ($\simeq$25 mV). Thus, $\psi_S^{max} = 8$ for a point charge and 4 for a plane. The equations for electrostatic interaction have been solved for a variety of geometries at least in approximation. For the interaction between two spheres, one obtains[17]

$$f = \frac{A_1 A_2}{x + A_1 + A_2} \quad (18)$$

Note that the asymptotic behavior of eq 18 is wrong; for point charges, $f = 1/x$ holds. Equation 18 simply becomes $f = A$ for a sphere against a planar wall. The latter was used to analyze the wall effect for a sphere in a cylinder in hydrodynamic chromatography[18,19] and for modeling the diffusion through membrane pores.[20] A modified function for this case is

$$f = \frac{A}{a} = \frac{R_\eta}{r} \quad (19)$$

Table III
Electrostatic Model: Fitting Parameters for Equation 29

	f	$\bar{f}$[a]	data	$\bar{a}$	$\bar{b}$	$\bar{r}$
planar wall	eq 19	$\frac{r-R_\eta-0.3I^{-1/2}\bar{x}}{r}$	all[b]	4.40	−6.32	0.976
			spheres[c]	1.64	0.58	0.583
cylinder cavity	eq 25	$\left(\frac{r-R_\eta-0.3I^{-1/2}\bar{x}}{r}\right)^{1/2}$	all	3.84	−5.14	0.983
			spheres	1.59	0.64	0.797
convex wall[d]	eq 18	$\frac{r-R_\eta-0.3I^{-1/2}\bar{x}}{3r+R_\eta+0.3I^{-1/2}\bar{x}}$	all	4.71	−1.78	0.972
			spheres	1.68	2.39	0.790
spherical cavity	eq 20	1	all	3.40	−4.19	0.987
			spheres	1.54	0.70	0.801

[a] Using $0.3I^{-1/2} = 1$ and a cavity radius of $r = 200$ nm. [b] All data shown in Figure 6. [c] Only the spherical viruses and thryoglobulin. [d] The cavity, radius r, between packed spheres, radius $\mathring{r}$, is $r = \mathring{r}/3$.

where r is the cylinder radius and $a = \kappa r$.[21] In analogy, a sphere A inside another sphere a gives

$$f = \frac{A}{a-A-x} \tag{20}$$

The interactions between charged rods have been studied as well.[22,23]

Finally we investigate the elaborate treatment of a sphere in a cylinder presented by Smith and Deen.[21] In our notation, the principal term of their eq 33 becomes our eq 16 if one sets

$$f = \frac{A}{a}\frac{I_0(a-A-x)e^{-(a-A-x)}}{I_0(a)e^{-a}[1-e^{-2x}g(a-A-x,a)h(A)]} \tag{21}$$

with

$$g(z,a) = \frac{e^{2(a-z)}}{a}I_0(z)\sum_{t=0}^{\infty}\frac{(z/a)^t(2t)!}{2^{3t}(t!)^2}I_t(z)\left[aK_{t+1}(2a) - \frac{1}{4}K_t(2a)\right] \tag{22}$$

and

$$h(A) = e^{-A}(e^A - e^{-A}) \simeq 1 \tag{23}$$

I_t and K_t are the modified Bessel functions of the first and second kind, respectively. Typical values for $g(z,a)$ are 10^{-5} for large pores and small solutes up to 10^{-1} for small pores and large solutes. This function is a correction term for strong electrostatic interaction. For $x > 1$, it may be ignored due to the e^{-2x} term. Further, we may write

$$I_0(z) = \frac{e^z}{(2\pi z)^{1/2}} \tag{24}$$

which is an excellent approximation for $z > 4$ and fair for $z > 0.3$ (for $0 < z < 0.3$, $I_0(z) \simeq 1$). Thus, eq 21 becomes

$$f = \frac{A}{a}\left(\frac{a}{a-A-x}\right)^{1/2} \tag{25}$$

Note that eq 25 converges to eq 19 only for $A \to 0$. For about $R_\eta > 0.62r$, the cylindrical model actually exceeds the limit of planar geometry ($f = 1$). The incorrect asymptotic behavior, $\lim_{R_\eta \to 0} \bar{x} = 0$, already occurs in eq 18.

For a cylindrical cross section, $x_r = r - R_\eta$, and combining eqs 12, 13, and 16 yields the equilibrium condition

$$\frac{n0.3I^{-1/2}}{r-R_\eta-0.3I^{-1/2}\bar{x}} = \left(1 - \frac{df(R_\eta)/dx}{f(R_\eta)}\right)V_e(\bar{x}) \tag{26}$$

which is best solved in logarithmic form. With eq 25, the logarithm of the first term of the right-hand side becomes $\ln(1-\epsilon) = -\epsilon$ with

$$2\epsilon = \frac{0.3I^{-1/2}}{r-R_\eta-0.3I^{-1/2}\bar{x}} \tag{27}$$

This should be compared to the error measuring the true equilibrium value $\bar{x}$, i.e.,

$$\frac{dR}{dI^{-1/2}} = 0.3\bar{x} = 0.3\bar{x} + 0.3I^{-1/2}\frac{d\bar{x}}{dI^{-1/2}} \simeq 0.3[\bar{x} - 1 - \epsilon(\bar{x}+1)] \tag{28}$$

which is $\bar{x}$ times larger. Theoretically the measured slope continuously decreases with decreasing I since $d^2R/d(I^{-1/2})^2 \simeq -0.3/I^{-1/2}$. If one keeps experimental conditions such that $R < 0.8r$, this nonlinearity will however be difficult to detect over the limited accessible range of ionic strength. Independent of size and charge then, $\bar{x} \sim \bar{x} + 1.7$ for our data where $\bar{x}$ is the experimental value defined by eq 10 and $\bar{x}$ is the corresponding theoretical value at $I = 90$ mM. $\ln \psi_S^{max}$ (see eqs 16, 17, and 26) may be considered constant for the data of Figure 6, leaving $\bar{x}$ at most 3% in error. Over the experimental data range $|d \ln \psi_S^{max}| \lesssim 0.05\ d \ln A$, an experimental fit of the data according to

$$\bar{x} = \bar{a}\ln(R_\eta\bar{f}) + \mathring{b}(\psi_{S1},\psi_{S2}) - \ln(0.3I^{-1/2}) = \bar{a}\ln(R_\eta\bar{f}) + \bar{b} \tag{29}$$

should yield $\bar{a} \sim 0.95$ as far as electrostatic theories go. $\bar{f}$ values are the product of entropy times f terms and are specified in Table III for the various geometries considered. That $I^{-1/2}$ term becomes a constant within the adopted experimental procedures, and its value (see above) will be reported as part of $\bar{b}$. For the cylindrical model

$$\frac{d\bar{x}}{d\ln R_\eta} = \bar{a} - \frac{1}{2}\frac{R_\eta/r}{1-R_\eta/r-0.3I^{-1/2}\bar{x}/r} \tag{30}$$

i.e., $\bar{x}$ reaches a maximum value somewhere above $R_\eta > r/2$ and then decreases again. Present and previous[2] experimental data of mine never exceeded this plateau. Note that the decrease of the slope in eq 28 is related to the predicted decrease in eq 30. Table III summarizes the coefficients of fitting the data to eq 29 using R_{SEC} in place of R_η. It also lists the correlation coefficients $\bar{r}$ for the various geometric models. All are properly linear, but none give the theoretically required factor $\bar{a}$. The analysis includes asymmetric molecules where the treatment as an equivalent sphere and the separation of shape from charge terms on the basis of this equivalent sphere may be questioned. Having ignored the ionic strength dependency of the intrinsic viscosity of DNA, the reported $\bar{x}$ values

might furthermore be biased (see Discussion section). However, even the more limited data range for spherical solutes alone gives slopes that are clearly too large.

In conclusion, other forces must be crucial in determining the average distance of closest approach. Solvation forces,[24] while crucial for neutral polymers (see Discussion section), may be neglected for our experimental conditions. Undulation forces[25] could in principle contribute in the case of flexible polymers. The similarity observed between DNA and viruses however suggests that undulation is of minor importance. Orientational forces,[26] suggested to influence SEC elution,[27] are present only in ordered gels and do not apply to SEC elution as demonstrated previously.[1] Thus, one is left to consider van der Waals attraction,[28] which for the interaction between a sphere and a plane reads[28-30]

$$V_w(x) = -\frac{1}{6}(H_o 2xe^{-2x} + H_\nu(x))\left(\frac{A}{x} + \frac{A}{x+2A} + \ln\frac{x}{x+2A}\right) \quad (31)$$

where H_o is the retarded zero frequency contribution to the Hamaker constant at $x = 0$ and H_ν the sum of the high-frequency contributions that are also a decreasing function of x at distances beyond 5 nm. The Hamaker constant depends on the chemical nature of the matrix, solute, and medium. The retardation effect has been explicitly calculated.[31,32] For distances (x) small compared to the dimensions of the surface, quantity in the second set of parentheses approaches $(A/x)^n$ with $n = 1$. For large relative distances, $n = 3$. Since the second set of parentheses increases with increasing R_η, while experimentally the contribution of van der Waals forces decreases with increasing R_η, the Hamaker constant itself, i.e., retardation effects, seems to be crucial unless $V_w(x)$ critically depends on the detailed geometry considered. Summing eqs 31 and 16 and inserting into eq 12, one obtains a very complicated function for $\bar{x}$ replacing eq 26, which is not simply transferred into eq 29. Small changes of R_η now may provoke large changes in $\bar{x}$. Quantitative judgements are premature; however, the equilibrium distance ($\bar{x}$) is clearly the result of a delicate balance between electrostatic and van der Waals forces. This is illustrated in Figure 8 for an arbitrary albeit representative case. Note that at large distances the van der Waals contribution actually decreases more rapidly than shown, which makes the secondary minimum even shallower.

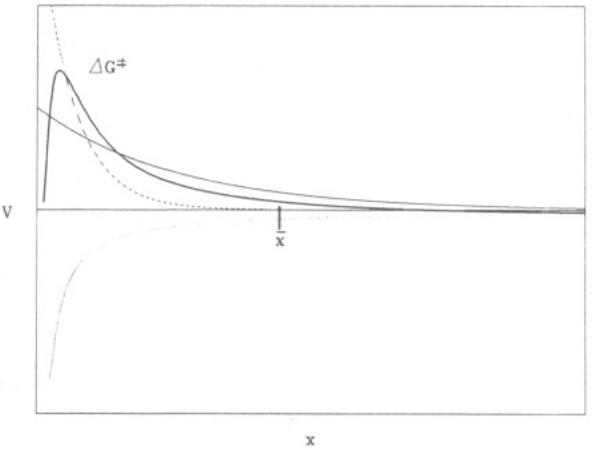

Figure 8. Energy diagram for the interaction between two surfaces as a function of distance of separation. The surfaces are assumed to be hydrophilic bearing charges of equal sign, and the refractive index of the medium is supposed to be lower than that of either surface. The average distance $\bar{x}$ which is measured in chromatography is defined thermodynamically by eq 12. Electrostatic repulsion (exponential decay) (—), van der Waals attraction ($1/x$ function) (···), solvation (exponential decay) (- - -), total energy (—). In close contact, there will always be an attractive minimum (primary minimum). Thus, in order to measure SEC elution, it is necessary that $\Delta G^\ddagger$ is sufficiently large. All other chromatographic modes (IEC, reversed phase, HIC) are stepwise processes of adsorption and desorption defined by ΔG_{bound} and $\Delta G^\ddagger$ and are thus fundamentally different from the SEC mode. Hydration forces are repulsive for hydrophilic (as shown) but attractive for hydrophobic surfaces, which will enhance binding. They are a strongly decreasing function of distance but notable even at 3-nm separation. Electrostatic forces become attractive for oppositely charges surfaces, again enhancing binding and creating a pronounced secondary minimum at a distance of several nanometers from the surface. Whether the secondary minimum is stable compared to the first depends on the remaining activation energy $\Delta G^\ddagger$, viz. entirely on solvation forces. The implications for theories of IEC are obvious.

Discussion

1. Universal Calibration. Following the original proposal of Benoit on the universal calibration of SEC in terms of $[\eta]M$, several studies in organic solvents (reviewed in refs 1 and 33) have confirmed this concept. Its mechanistic origins are still obscure. It has become routine to polymer chemists even though adsorption effects confound the mechanism proper in organic solvents.[34] However, some investigators still prefer calibrations in terms of the radii of gyration, which is implied in the Coll–Prusinowski approach.[35] In aqueous solutions, matters are different. First of all, diffusion coefficients are in continued use in the biological sciences and only lately have there been reports that question this approach. Finally there have been a number of theoretical treatments all arriving at yet different functionalities, none of which were borne out by recent experiments.[1,3] Extensive literature exists regarding charge effects in the chromatography of polyelectrolytes (reviewed in ref 2). There seems to be general agreement that universal calibration as originally devised is a concept too limited to account for the full body of phenomena. A confusing wealth of pertinent information has accumulated over the years on the issue of universal calibration in aqueous SEC,[1-3,27,36-61] and it seems warranted to bring the issues to the following points: comparison of different matrices (for a survey of commercially available SEC columns, see ref 62); comparison of different flexible polymers largely to explore artifacts of adsorption but also geared to verify the $[\eta]M$ measure; comparison of neutral polymers with polyelectrolytes under conditions of sufficiently high ionic strength supposed to screen any charge-related effects; and finally the role of the shape of the molecules.

Overview. The reviewed studies cover major column brands: porous glass and silica (CPG,[42,55,58] Spherosil,[57] CPG/Fractosil mixed beds,[60] Spherosil/Fractosil mixed beds[52]), derivatized silica (TSK SW,[1,2,44-48,54,59] μBondagel,[43,45] Protein-WS,[55] Zorbax I-250,[1,2] Spherosil QMA[40]), macroreticular polymers of the microparticulate type (TSK PW,[1,2,38,39,41,49-51,55,63,64] OHpak B,[55] Ultrahydrogel,[56] Mono S[2]), and those of fibrous porous networks (Superose,[1-3] Sepharose,[27,36,54] Sephadex,[37,50,54] amylose gels[53]). Other commercially available SEC columns have been characterized only superficially or not at all. In the following, SEC elutions of different types of polymers will be compared on the basis of viscosity radii under conditions where differences in the interfacial effects presumably may be neglected, i.e., for polyelectrolytes at high ionic strength (usually $I = 0.1$–0.2 M). Several molar concentrations of salt generally favor adsorption following Hofmeister's lyotropic series (hydrophobic interaction chromatography

(HIC)). Whenever a polymer was reported to elute delayed, even below 1 M ionic strength, it will be listed to adsorb even though some intermittent I may be found where coincidental congruent elution with other polymers is observed. With few exceptions, a whole series of different sizes has been studied for each polymer type. It must be emphasized that the current report is exclusively devoted to solutes at infinite dilutions, i.e., to the properties of an isolated molecule interacting with the matrix and solvent mixture but never with twin macromolecular solutes. Reported literature seems to belong to this domain, but the issue is rarely addressed explicitly.

Dextran, PEG, and Pullulan. The compounded evidence suggests that dextran does not adsorb to most of the columns studied[38-46,49,51,56,58,59] except for one report on underivatized porous silica[57] (however, it does not adsorb to porous glass[42,58]). On the chemically homologous Sephadex, it elutes later than PEG[37,50,54] but together with native spherical proteins,[54] thus rejecting the involved interpretation of ref 37. Lack of data makes a decision for agarose difficult.[36] A similar convenient reference compound of the coiled structure type is pullulan without any reports of adsorption.[3,39,42,43,49,51,55] The third neutral coiled polymer reference is PEG, variably called poly(ethylene oxide) for the larger homologues,[37-41,46,49-51,54,56,59,64] which adsorbs to Waters I-125[39] and in fact to most bonded silica phases.[65] For unknown reasons, PEG elutes consistently earlier on Sephadex than dextran or proteins,[37,50,54] One of these authors reported the same for TSK PW;[50] however, this result may be dismissed in light of five other independent studies on TSK PW that demonstrate congruent elution of dextran and pullulan and PEG.[38,39,41,49,51] PEG elutes according to R_η on TSK SW,[46,59] on Spherosil QMA,[40] a quaternary methylammonium cationically coated silica column, and on Ultrahydrogel.[56] Other matrices have not been studied. A most interesting aspect of the Spherosil QMA study[40] is the ionic strength dependent elution of dextran as well as PEG even though intrinsic viscosities were measured for each eluent. In fact, its variation was found to be negligible contrary to the claim that dextran is prone to aggregate in pure water.[65] Salts are reported to bind to PEG and contract its conformation,[66,67] but this should have been taken care of by using appropriate $[\eta]$ for each solvent. Dextran and PEG might also have adsorbed or this particular column changed porosity depending on I. The latter possibility will be given special attention below. Ionic strength dependent elution was also observed for PEG of $R_\eta < 1$ nm on TSK PW but not for larger PEG. However, $[\eta]$ was not measured in each eluent.[41] With TSK SW, elution of dextran was independent of ionic strength from $I = 0$ to 0.5 M.[44] While clearly establishing the absence of adsorptive non-SEC effects, all these comparisons do little to qualify universal calibration in terms of viscosity radii. It had been erroneously suggested that $R_\eta = R_S$ for PEG as well as dextran[50] and that calibration in terms of R_G works equally well for the set pullulan = dextran = PEG.[49] In fact, another study reported calibration of dextran = pullulan in terms of R_G without even mentioning R_η.[43] Thus, universal calibration may only be tested by comparing polymers of widely different structure, i.e., coils, spheres, and rods.

Other Probes. First, however, the list of compounds enrolled in these comparative studies shall be completed. PVAl elutes congruently with PEG on Sephadex according to R_η but earlier than dextran;[37] PVP2 congruently elutes with PVP4, PLys, NaPSS, dextran, and PEG on Ultrahydrogel[56] but strongly adsorbed to μBondagel.[45] PVP2 also adsorbs to TSK SW[45] although coincidental congruent elution is reported for intermediate ionic strength, the same that was exclusively studied on Ultrahydrogel.[56] PVAc congruently elutes with PDMDAAC, dextran, PEG, and proteins on TSK PW,[41] whereas PVA adsorbs on TSK PW.[41] The feasibility of studying cationic polymers on TSK PW was independently suggested, however, without in-depth analysis.[63] PEI congruently elutes with dextran on TSK SW[45] but is adsorbed on μBondagel[45] and TSK PW.[41] PVPn congruently eluted with dextran on Sephadex but later than PEG.[37] On TSK PW, PVPn was compared to PEG, albeit in methanol–water mixtures containing salt, and was found to elute congruently.[64] PVPn adsorbed to virtually all bonded silica phases studied,[65] including Spherosil QMA.[40] PLys, on the other hand, congruently eluted with PEG and dextran on Spherosil QMA,[40] but this was also achieved on Ultrahydrogel.[56] Amylopectin and chitosan (which adsorbed at high I) were also studied,[40] but the data are inconclusive. Amylopectin and amylose were, however, successfully studied on TSK PW where they eluted congruently with pullulan = dextran = PEG.[51] Pectin eluted prematurely on Sepharose compared to dextran.[36] PVP2 was also studied on a noncommercial cationically derivatized CPG material and eluted earlier than dextran even at $I = 0.2$ M.[61] Maybe dextran became adsorbed. The same derivatization was applied to Lichrosorb, but data were inconclusive since the column deteriorated.[45] Since all regular SEC columns contain residual anionic charges and are polar, chromatography of cationic and hydrogen-bonding polymers poses a great challenge. To minimize these effects, other cationically derivatized columns or special materials are being developed and marketed but none has been thoroughly characterized. Proprietory matrix properties unfortunately also prevent a rational analysis of this issue. But even with polyanions, problems may arise: NaPSS congruently eluted on Ultrahydrogel with a number of other polymer types,[56] and also on Spherosil[57] and on CPG.[42,55,58] On TSK PW, one study reported adsorption[55] and another congruent elution with PEG and dextran in 0.42 N NaOH.[38] On OHpak B[55] and Protein-WS,[55] it adsorbed. NaPAA[58] and its copolymer with ethyl acrylate[58] as well as NaPGlu[57] congruently eluted with NaPSS and other compounds on porous glass and silica, respectively. Heparin eluted earlier from TSK SW than PEG = dextran,[46] and it remains to be determined whether ionic strength was too low or whether true deviation from R_η calibration occurred. Heparin is a rather expanded coil having a Mark–Houwink exponent of ~1, i.e., similar to NaPSS,[46,56] but is clearly not a stiff rod. Xanthan was originally reported to elute earlier than predicted by R_η,[52] but later studies indicate that the R_η universal calibration is fulfilled.[68] The Mark–Houwink exponent of xanthan depends on ionic strength[69] and is similar but slightly less than that of DNA. Both heparin and xanthan may become crucial subjects for assessing universal calibration. All together, the outlined chemical details provide important clues for the present concerns besides the issue of adsorption: The congruent elution of a variety of chemically different polymers according to their viscosimetric size (R_η) implies that whatever interfacial effects (solvation!) contribute additionally to R_{SEC} seem to be independent of the variable chemical nature of the macromolecular surfaces.

Universal Calibration. The first critical test of the universal R_η calibration came from comparing compact spheres with coils in 1982/1983. Globular proteins were compared to dextran, PEG, and other coiled polymers on

TSK PW, and elution was found to be congruent.[41] On TSK SW, proteins eluted congruently with dextran according to R_η but not by R_S,[44] superseding an earlier crude study on TSK SW that did not discriminate between R_S, R_η, or R_G.[59] Lately it was shown that proteins congruently elute with pullulan on Superose[3] and with dextran on Sepharose.[54] Within errors of measurement proteins, dextran and pullulan congruently eluted on amylose gels.[53] A somewhat indirect assessment was done with polystyrene latex spheres on a CPG/Fractosil mixed bed column.[60] Aqueous SDS containing solutions of latex was measured at low ionic strength and elution volumes extrapolated to high I as a linear function of $I^{-1/2}$ to eliminate interfacial effects. A direct measurement at high I was impossible since latex irreversibly would adsorb. Conversely, my data show that linear extrapolation is obtained with radii but not with elution volumes (see below), making the obtained values somewhat uncertain. These values were then compared to polystyrene coils measured in tetrahydrofuran on the same column, conditions that need not exhibit the same solvation related interfacial effects (see below). Nonetheless, it was found that coils and spheres congruently elute according to R_η. In another study, proteins were denatured in 6 M GuHCl where they form rather ideal coils. These were found to congruently elute with native globular proteins according to R_η on TSK SW[47,48] and Sepharose.[54] Globular proteins and viruses were also compared to rod-shaped proteins and viruses varying from extended coils to stiff rods on TSK SW, TSK PW, and Superose, and elution was found to be congruent for R_η.[1] Claims conflicting with this statement will be discussed below. Unfortunately some of these proteins are difficult to handle (see below) and DNA seemed to be a natural choice for further comparisons.

2. DNA. SEC studies are limited. The technique was used for removal of low molecular weight contaminants such as linker oligomers, enzymes, and ligation products[70,71] as well as for removal of chromosomal DNA and RNA from plasmids of interest,[72-80] for demonstrating the feasibility of plasmid and restriction fragment separation,[81-90] fractionation of sonicated[13] or DNase degraded[12] DNA, for a Hummel-Dreyer dye binding experiment to DNA,[91] for RNA selection via RNA/DNA hybrids,[92] and for chromatin preparation.[93] The chromatographic dimension R_{SEC} for DNA, first claimed to elute congruently with proteins and viruses according to R_η in 1987,[1] was later shown to appear larger than R_η for short DNA but was believed to converge to the congruent R_η calibration for large sizes that could be considered coiled.[3] Consequently, the present report studied in detail the size range of 150–2200-bp DNA on a TSK 6000 PW column. Its upper useful size limit is about 10 000 bp,[90] but beyond the size of 3000 bp, reference compounds were not available. Materials suited for still larger DNA, while feasible, are currently not available. Shear degradation of the studied DNA was not observed. It was found that based on the universal R_η calibration with viruses all R_{SEC} values for DNA are about 10% larger than the corresponding R_η values if the latter are taken from the intrinsic viscosity data of Eigner and Doty.[7] This is a small difference compared to the effects discriminated in the previous publication,[1] which therefore omitted any involved debate of the uncertainities in the available DNA reference data. Thus, it was not explicitly mentioned that the reported s values were up to 10% smaller than what has become the standard reference set. Chromatographic elution radii, on the other hand, were found to be larger

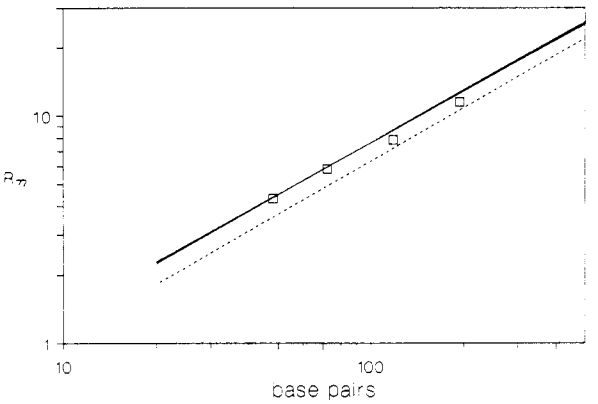

Figure 9. Elution volumes of DNA reported by Dubin and Principi[3] for a Superose 6 column (Pharmacia) converted to chromatographic radii according to the calibration line for pullulan and globular proteins in a procedure analogous to the treatment of our data (□). The regression lines obtained from our data and calculated with eqs 3 and 5 are shown for comparison (—). Dubin and Principi used the Mark–Houwink coefficients reported by Eigner and Doty (eq 1) (- - -). They consequently concluded that DNA does not elute according to universal calibration.

than calculated from the reference $[\eta]$ values by the same amount. It thus seemed acceptable to imply universal calibration principles also for DNA since clearly the Stokes radius, radius of gyration, mean linear extension, or virial coefficients had been ruled out.

Figure 9 reevaluates the data of Dubin and Principi,[3] identical with the data handling for Figure 3. It demonstrates that the latter data, obtained on TSK PW, perfectly extrapolate to Dubin's data for smaller sized DNA, measured on Superose. Thus, the chromatographic Mark–Houwink relationships (eqs 3–6) are generally valid for DNA regardless of the type of chromatographic matrix and the size and origin of DNA down to at least 50 bp. The apparent deviation from conventional intrinsic viscosities (eq 1) furthermore does not seem to be related to persistence length as judged from comparison with TMV (for additional considerations, see below). Thus, the problem either reflects interfacial phenomena or simply is due to inappropriate Mark–Houwink coefficients in the literature. Ionic strength related double layer size effects have been ruled out experimentally, and different extents of hydration of DNA vs proteinacious surfaces, while conceivable (see below), clearly put the vast number of chemical studies reported above in limbo. Final judgement thus should await the redetermination of the intrinsic viscosities of monodisperse preparations of DNA restriction fragments to exclude the possibility that any conclusions be mislead by errors in the presently accepted reference data.

The Mark–Houwink coefficients for DNA depend on size and ionic strength. Equation 1 applies for DNA around I = 200 mM and below 3000 bp where it forms flexible rods that alternatively may be viewed as rather expanded elipsoidal coils. The Mark–Houwink exponent for large DNA (about 3000 bp) is 0.7, closer to an ideal coil.[7] For large DNA, the ionic strength dependency of intrinsic viscosity, calculated from experimental data on Bacteriophage T2 and T7 DNA,[94] is

$$[\eta] = [\eta]_\infty + 1.9 \times 10^{-3}[\eta]_\infty^{1.4} I^{-1/2} \qquad (32)$$

where $[\eta]_\infty$ is the intrinsic viscosity at infinite ionic strength and units are mL g^{-1} and mol. Other data suggest that swelling of DNA is less than half as large.[95] In comparison, ionic strength related swelling of many typical polyelectrolyte coils is larger by an order of magnitude.[95] Few

hydrodynamic studies concerned small DNA, which is inherently more expanded and thus should be less sensitive to ionic strength related swelling. By using eq 32 as an upper bound, the viscosity radius of the 2217-bp restriction fragment could be up to 8% larger at I = 10 mM than at I = 200 mM. For the 156-bp DNA, the equivalent difference is only 2%. Between I = 60 and 200 mM, the effects are 5-fold smaller and may be ignored altogether in line with experimental evidence (eqs 3–6).

In terms of application, SEC lacks the resolution of electrophoresis, and repeated usage of equipment may introduce deleterious cross-contamination in some preparative applications. Whenever column chromatography is feasible, many chores are better served by preparative SEC rather than IEC. Analytically it provides accurate information on DNA size and generally holds great promise for hydrodynamic characterization. Linear, supercoiled, and circular nicked forms of the same DNA sequence bear different radii and thus elute differently (unpublished observations and refs 76 and 78). Finally, it will be particularly interesting to characterize bent or other unusual DNA by this method.

3. Lipids and Surfactants. Chromatography of or in the presence of lipids and surfactants deserves special consideration. Firstly, adsorption to the matrix may be more critical; secondly, ternary systems are bound to exhibit differential solvation which may change the nonelectrostatic interfacial separation effects (discussed below); thirdly, reference data for these systems are still ill-defined; and lastly, these complex systems play a prominent role in the contemporary debate of universal calibration.

Micelles and Vesicles. Micelles, as an interactive system, require eluents that are ideally identical with the sample[96] unless one explicitly wishes to study kinetics and equilibria amongst the various interactive components. SEC of micelles has been reviewed by Birdi[97] without addressing the issue of universal calibration. The latter aspect has been studied on Sepharose.[98] Biogel A,[99,100] Superose,[100] Sephadex,[54] and agarose[54] with converging R_{SEC} values but contradicting conclusions originating from differences in the reference data. It thus seems premature to draw conclusions upon the mechanism of SEC. Vesicles of various sizes and composition have been studied in lipid saturated columns (TSK PW and Sephacryl),[101] but comparison to other types of materials is lacking. Convergent calibration in terms of particle diameters (electron microscopy) was reported for proteins and lipoproteins on TSK SW and TSK PW.[102]

Protein–SDS Complexes. SEC analysis of protein–SDS complexes, which form expanded flexible coils,[103,104] is an issue on its own. Tanford's group originally found on Biogel A that protein–SDS complexes and proteins in GuHCl congruently elute according to R_η.[105] Later, on Sephadex, they instead employed an average between R_S and R_η for comparing protein–SDS complexes with native proteins.[106] Yet later, on Sepharose, they observed that large protein–SDS complexes elute later than even predicted by R_S.[27] On CPG, others found that protein–SDS complexes elute according to R_S.[107] An earlier study[108] had introduced a novel measure, exclusion sizes, whose implications will be discussed below. On TSK 3000 SW, small complexes (R_η < 7 nm) eluted slightly prematurely on the basis of R_η.[48] This was later confirmed,[54] while a third study did not attempt universal calibration.[109] Large complexes seemed to elute increasingly delayed,[54] and they definitely eluted later on Sepharose 4B, which cannot reliably measure the smaller ones.[54] Surprisingly, the latter authors did not observe the ionic strength dependency of elution reported previously for protein–SDS complexes on TSK 3000 SW[48,110,111] and expected by the general principles outlined in the present report. Evidence for late elution of protein–SDS complexes thus heavily depends on two independent studies of the same matrix, Sepharose, and is opposed by compelling evidence that rodlike molecules elute according to R_η or even slightly earlier than that (refs 1 and 3 and the present report). The protein–SDS system is extremely complex since bulk intrinsic viscosities, chromatographic retention, and the amount of bound SDS depend on ionic strength and SDS concentration[103,110,112–114] (see also refs 48 and 111). One study claims that only the surfactant monomer concentration matters.[115] This concentration depends on I via the critical micelle concentration. Furthermore, delayed SEC elution was observed at high ionic strength, introducing hazards of adsorption,[110,116,117] and peak broadening at high I indicates the same.[111] The shape of the protein–SDS complex itself appears to be unrelated to the sequence and structure of the native protein and unrelated to the α-helix content of the protein–surfactant complex.[103,118] However, glycoproteins elute unpredictably in SDS,[119,120] and membrane proteins, which are aberrant in SDS–PAGE,[113,121] apparently have not been studied. Since electrophoretic mobilities of SDS–polymer complexes are virtually independent of molecular weight but strongly depend on the amount of SDS bound,[113,122] SDS–PAGE generally seems more susceptible to anomalous migration. The Mark–Houwink coefficients of the intrinsic viscosity of protein–SDS complexes are almost identical with those of native linear double-stranded DNA. Their SEC elution seems, however, to be exceedingly different. Clearly more work will be required to elucidate this interesting system.

Membrane Proteins. Finally, surfactant-solubilized membrane proteins have been studied in the presence of a variety of surfactants by Le Maire et al. on Sepharose,[123] Sephacryl,[123] Sephadex,[54] BioGel A,[54] TSK SW,[124] and TSK PW.[124] With the exception of TSK PW, where they elute later than expected even by R_S, suggesting adsorption, their R_{SEC} values are independent of the type of matrix and typically 20% (range 5–50%) larger than R_S. Styring et al.[125] have observed that surfactant-coated latex spheres exhibit intrinsic viscosities about 40% larger than expected from the spherical nature were R_η should equal R_S. Thus, the observations of Le Maire et al. are principally consistent with universal calibration in terms of R_η albeit details remain to be carefully checked by measuring intrinsic viscosities in each case.

4. Focal Issues. Summarizing all available evidence, there seems to be a converging consciousness but not yet a consensus on SEC calibration principles. This favors continued segregation into discipline-specific traditions for calibration, followed by a majority of chromatographers who are practical and not concerned with principles. While occasionally appropriate in limited applications, this negligence has created false claims and certainly has deterred many authors from even bothering with the maze of published literature. A critical focus on the key issues is therefore indispensible.

To start with, the terms of analysis should be clarified. Hydrodynamic radii are mathematical constructs that define an equivalent sphere to represent an arbitrary shape that is rotationally averaged by variable criteria; e.g., diffusion gives a different average than viscosity and the chromatographic process may as yet be different. Knowing the type of averaging, inference about the physics of the

process may become possible. The concept of radii, preferred by the present author, entails some geometric intuition for the analysis of interfacial effects, and it actually turned out to provide a simple separation of variables in eq 9. Viscosity radii (R_η) are strictly equivalent to $[\eta]M$, the more commonly used term for universal calibration, and both terms are related mathematically by eq 2. The suggestion[126] that R_η should not be used since it was merely an approximation to $[\eta]M$ is simply incorrect.

Waldmann-Meyer[107,127] presumes, in line with a widespread notion, that permeation of the matrix is a diffusion process that makes R_S the only natural choice as a shape function. However, the mechanism of SEC is not unequivocally resolved. One may actually reverse the point: given that calibration relates to a rotational average that closely follows the rules of intrinsic viscosity rather than diffusion, does this mean that convective features are involved? Since dispersion does not parallel the large variation of retention that is due to interfacial effects,[2,128] dynamic processes, however, are clearly not rate limiting. For this reason, an equilibrium model has been adopted in the present paper. Convection, however, certainly is crucial for dispersion, especially with larger pores, a fact debated in detail previously[1] and picked up recently.[129] Whether convection also is responsible for the viscosity-like rotational average observed in chromatography is a complicated detail. Due to limited space, a thorough consideration of dispersion and the mechanism of SEC is forthcoming separately.[128] The strongest experimental point in Waldmann-Meyer's preference for Stokes radii is his claim that elution of protein–SDS complexes follows R_S. While there is clearly a problem with the R_η calibration of this system, accumulated evidence also rejects R_S. Unfortunately, the nature of this system is ill-conditioned (reviewed above) and requires urgent clarification. Well-characterized rods in aqueous systems lacking complications from surfactants have been shown independently to appear at least as large as predicted by their viscosity radii.[1,3] The final argument of Waldmann-Meyer is the supposedly good agreement between mercury porosimetry and inverse chromatography based on R_S. Collins and Haller[108] previously, however, reported chromatographic exclusion radii for small protein–SDS complexes based on pore sizes determined by mercury intrusion that are about 3 nm larger than the corresponding viscosity radii. Since $R_{SEC} < R_\eta$ for the larger protein–SDS complexes, the reported decrease of this number with size based on R_η could be an artifact. For dextran, the comparable difference increases from less than 1 nm for $R_\eta \sim 3$ nm to about 6 nm for $R_\eta \sim 20$ nm, reproduced in two studies.[130,131] According to universal calibration reviewed above, these numbers should be the same for all solutes regardless of charge and chemical nature. These differences are principally anticipated due to interfacial effects (see below). Their magnitude may, however, be even larger because the real pore sizes may be larger. Mercury porosimetry does not give mean but minimal pore sizes whenever diameters are irregular.[132] Electron microscopy of CPG, the matrix referred to, clearly demonstrates highly irregular interconnecting pores of varying diameter, all but cylindrical and with larger diameters than derived from mercury intrusion.[133] Thus, these data may be insufficient to support preference of R_S above R_η.

Le Maire and collaborators have reported numerous observations regarding membrane proteins, micelles, protein–SDS complexes, and also surfactant-free asymmetric molecules. Most of their chromatographic experiments have been confirmed. Premature elution of PEG seems to be matrix specific (discussed above). Regarding micelles, their interpretation differs from others due to a different choice of reference data (discussed above) which first needs to be settled. A novel proposal to explain their data on membrane proteins has been advanced above. A satisfying interpretation for the observed elution of protein–SDS complexes (also discussed above) remains to be given. Their conclusions regarding late elution of fibrinogen and tropomyosin compared to globular proteins[54] are doubtful as follows: Both materials were obtained in lyophylized state from Sigma. I have previously reported that this tropomyosin from Sigma is not structurally competent. It not only elutes later from SEC than native tropomyosin but also exhibits decreased Stokes radii in quasielastic light scattering.[1] Their elution position for tropomyosin, which agrees well with values found previously for material from this source,[1] thus may not be taken for the properties of native molecules and their viscosity radius. In light of such experimental difficulties, data on fibrinogen similarly demand controls. In conclusion, delayed elution of rod-shaped structures, which reiterates Tanford's idea of end-on insertion[27] that was previously dismissed,[1] cannot be supported by the presented evidence. It is independently contradicted by Dubin and Principi, who rather claim the reverse, i.e., premature elution of stiff rods.[3]

Dubin and Principi[3] reported that $R_G \gg R_{SEC} \geq R_\eta$ in the absence of wall effects. While the classical universal calibration holds for flexible coils and spheres, i.e., $R_{SEC} = R_\eta$, premature elution was observed for stiff rods shorter than their persistence length. The present reinvestigation of DNA, however, reveals that premature DNA elution is independent of size and stiffness and that in comparison TMV, which is much stiffer, elutes properly by R_η. To ultimately settle this point, it would be highly desirable to have available spherical particles of about 80-nm radius that may be studied in the absence of surfactants. It is, however, very likely that the reference intrinsic viscosities used for DNA are in error, and these need to be redetermined first. Xanthan, being structurally similar to DNA, elutes according to R_η.[68] Even larger deviations have been reported[3] for the extremely stiff rod schizophyllan ($b = 1.66$) than for DNA ($b \leq 1.3$). TMV and its dimer are also extremely stiff. If their intrinsic viscosities are expressed in terms of a Mark–Houwink relationship, the exponent becomes $b = 1.75$, which is close to the theoretical limit for infinitely stiff rods ($b = 1.80$).[134] The fact that both elute later than DNA on the basis of eq 1, i.e., they might actually elute congruently according to R_η, strongly suggests that further comprehensive studies of schizophyllan, in particular of larger homologues, are necessary.

5. Interfacial Phenomena. SEC separates molecules according to the total volume in the column that is accessible to the molecules' center of gravity. This reciprocally means according to the distance of closest approach of the center of gravity from the walls of the porous matrix. SEC thus inherently operates on the basis of interfacial effects.

General Definition. Macromolecules too should be considered to have a wall whose exact location may be subject to debate. Are slowly or nonexchanging solvent molecules or tightly bound counterions part of the body, i.e., inside the contour interface? For the surrounding medium, the wall represents the properties of the body, and solvent perturbation does not need to consider the detailed volume behind the wall inside the body. Con-

sequently, charges are normally considered to be located at this interface. The total distance of closest approach may then be written for a given particle orientation φ,θ

$$R^{\varphi,\theta} = R^{\varphi,\theta}_{body} + R^{\varphi,\theta}_{if} \quad (33)$$

where "if" stands for the interfacial separation between the two interfaces. To obtain the average exclusion distance, which is the parameter measured in SEC, one must average over all orientations of the arbitrary particle

$$R = \langle R \rangle_{\varphi,\theta} = \langle R_{body} + R_{if} \rangle_{\varphi,\theta} = \langle R_{body} \rangle_{\varphi,\theta} + \langle R_{if} \rangle_{\varphi,\theta} = R_{SEC} + R_{IF} \quad (34)$$

The separation of variables in eq 34 is nontrivial except for spherical particles. Both resulting terms are themselves a function of solvent conditions, in particular of the ionic strength for which eq 9 is a special case. A priori, the rotational average of a particle opposite a wall need not equal any other known measure, each one being the consequence of a particular process, e.g., scattering leads to R_G and hydrodynamics to R_S or R_η depending on whether the particle diffuses in a solvent or moves with the solvent. By definition, R_{SEC} changes with conditions only if the position of the solute contour interface changes. If $R_{SEC} \neq R_\eta$, it becomes difficult to define its ionic strength dependency, but it will parallel changes in R_η.

Experimental Data. For the proteins and viruses studied previously[2] and here, R_η is independent of ionic strength. R_η of DNA is almost but not entirely independent of I. Analysis of data according to eq 9 using a constant R_{SEC} value thus introduces some bias in $\bar{x}$. If eq 32 would apply for small DNA, its correction amounts to

$$\bar{x}_{true} = \bar{x} - 5 \times 10^{-3}(R_\eta^\infty)^{1.4} \quad (35)$$

i.e., the bias would increase from a negligible value of 0.1 for 156-bp DNA to a possible 2.3 for 2217-bp DNA. Uncertainties in eq 32, discussed above, might reduce this range to below 1.0 for 2217-bp DNA. Real data for small DNA are altogether lacking, and the actual extent of hydrodynamically operative expansion is unknown. It was thus decided to present $\bar{x}$ data of DNA uncorrected for the time being (Figure 6). Data in the size range of spherical viruses are effectively unbiased anyway. Those of the size of TMV, however, may not match the $\bar{x}$ value of the latter as well as suggested by Figure 6. Linearity of eq 35 does not hold for large coil expansion, and one should generally determine a true $\bar{x}$ directly from plotting $R - R_\eta$ vs $I^{-1/2}$ where R_η is either taken from an equation similar to eq 32 or directly from experiment. Note that it is always possible to extrapolate R values independently to the ionic strength of universal calibration and thus obtain a hydrodynamic radius for the latter conditions that might not themselves be experimentally accessible.[15] The chromatographic dispersion depends on the hydrodynamic size but not on R_{IF},[2] and thus R_η may be independently derived from the same experiment. Whether this ever becomes practical remains to be seen. For polydisperse samples, apparent dispersion increases with increasing I due to greater selectivity,[55,125] i.e., a flatter gradient $d \ln R_{(\eta)}/dV$ (mL), and this may hide variations of R_η. Many investigators have used $I^{-1/2}$ dependency of V (mL)[55,125,135-137] rather than of calibrated R, which makes their data depend on the selectivity profile, i.e., pore size distribution. The experimentally observed linear dependency of R_{IF} on $I^{-1/2}$ implies curvature if the same data are plotted by V (mL) unless particular curved calibration graphs circumstantially make them appear linear. Theoretically, linearity is not expected except for fortuitous cancellation of terms, but data will appear linear within present experimental uncertainties over the limited experimental range of ionic strength accessible in SEC. Equation 9 is thus merely an useful approximation for certain experimental conditions, and more general situations should refer to eqs 11 and 12 for defining R_{IF}.

Other Investigators. A similar analysis of wall effects was done by Small[138] for capillary hydrodynamic chromatography of latex spheres. For a mean particle radius of about 100 nm, he reports a thickness equivalent to $\bar{x} = 27$. Contrary to my observations and analysis presented in the Results section, this value is attributed entirely to electrostatic repulsion. van der Waals attraction is only believed to be responsible for adsorption (via the secondary minimum) at higher ionic strength and larger particles. The present logic of analyzing SEC elution has also been previewed by Styring et al.,[139] but no detailed experimental account was given. Dubin et al.[42,140] followed the same main logic but took an entirely different route to analyze charge-related wall effects. Repulsion distances were measured under assumptions about the geometry of pores at one ionic strength for a series of homologous flexible polymers (NaPSS) rather than assumptionless via universal calibration for each polymer individually at a series of ionic strength as done here and in the previous report.[2] Dubin notes, however, that charge effects are size dependent. For CPG and a mean size of $R_\eta \sim 5$ nm, he obtains a reduced repulsion distance of $\bar{x} = 2.6$[62] with $\bar{x}$ actually decreasing slightly with increasing ionic strength. This is quite possibly a real effect (see Results section) and could be overlooked by my mode of data analysis as long as the curvature is small. NaPSS presumably is maximally charged, but the charge of the CPG matrix is unknown. However, it was previously shown that different matrices vary only within a factor of 2. At this level of comparison, Dubin's data are consistent with mine for TSK PW, Mono-S, and Superose.

Hydration Forces. The protracted quest for universal calibration generally either assumed hard core bodies, i.e., rectangular potentials at the interface implying $R_{IF} = 0$, or implied that charge-related effects vanish at high ionic strength with the same consequence. They did not concede that once electrostatic interactions were proven to be crucial, any interfacial energy would contribute similarly. Superficially, the issue of universal calibration thus concerned the mode of rotational averaging; practically congruent elution is only found if R_{IF} is equal for all solutes of same size whatever its exact value. The exact value, however, needs to be considered for inverse chromatography,[2,132] which compares R to pore size. By such a comparison, a value of $R_{IF} \simeq 3$ nm was found for a coiled polyelectrolyte ($R_\eta \sim 3$ nm) at high ionic strength on CPG.[108] Using non-chromatographic methods, Parsegian et al. have identified hydration forces that based on eq 12 cause some minimum 3-nm separation. Judged by different cut-off criteria the hydration layer has been quoted to be 1–2 nm thick.[24] Little is known about the role of geometry and size on solvation forces. At physiological ionic strength ($I \simeq 170$ mM), DLVO forces of a typical enzyme ($R_\eta \sim 3$ nm) amount to $R_{IF} \simeq 3$ nm, less for lower charge densities. They are 4-fold larger for the largest structures studied (Figure 6). It was such large structures that hydration forces have thus far been measured for, and this suggests that R_{IF} for large structures is still dominated by electrostatic repulsion. Congruent elution with non-electrolytes then should be observed for the smaller macromolecules, as is indeed the case (reviewed above), but not for the very large ones. Note, however,

that $R_{if} \gtrsim 6$ nm for large dextrans[130,131] (see above), which is comparable to DLVO forces of similar sized polyelectrolytes at physiological ionic strength. It certainly seems intriguing to utilize SEC in developing physical models of solvation and systematically investigate the detailed properties of colloidal surface forces with tailored porous matrices. Certainly the proposal that the unexpectedly large hydration forces are due to Coulombic interactions on zwitterionic surfaces[141,142] must be put into question. Differences of solvation, however, are to be expected for different solvents and in particular solvent mixtures of varying ratios (see ref 2). In hydrodynamics, the shear plane usually includes a monolayer of solvent that is commonly expressed as the degree of hydration in g of H_2O/g[1] and is thus much less than the actual range of solvent perturbation.

Geometry of the Matrix. The actual geometric setup of a solute in a pore is complex, is variable, is largely unknown, and may depend on the size of the solute relative to the pore. Judging by electron microscopy of CPG,[132,133,143] fused silica,[132,144-146] styrene–divinylbenzene copolymers,[147] methacrylate (Spheron/Separon),[148] TSK PW,[149] Sephacryl,[150] and agarose[132,151-153] all are totally porous, i.e., they contain interconnected flow-through capillaries rather than dead-end pores. For Haller's CPG, a cylindrical tube seems appropriate (i.e., a geometry with spheres inside a cylinder). Pores of macroreticular matrices of the microparticulate type as well as those in fused silica beads are formed by agglomeration of microspheres (nodules), i.e., by convex surface elements, and a sphere–sphere model might be the most appropriate for small solutes while larger ones may primarily sense some sort of cylindrical enclosure. Fibrous porous networks, on the other hand, would demand a hybrid geometry of spheres outside of cylinders, which themselves form some hypercylindrical circumferential assembly within which the sphere is confined. For nonspherical solutes, the mathematical challenge becomes unlimitedly more complex. Table III shows that electrostatic interactions depend somewhat on the presumed geometric setup (see Results section). These results also demonstrate that electrostatic considerations alone are insufficient to explain the observations, and a full DLVO treatment is necessary. Actual DLVO separation distances crucially depend on van der Waals forces, and comparatively little is known theoretically about their geometric dependency, which may be large. Increasing theoretical effort thus needs to be directed to analyze van der Waal forces in varying geometries and for large distances where retardation of forces becomes crucial. Generally, attractive van der Waals forces may also become repulsive.[28] As a practical consequence, SEC of neutral polymers may be greatly improved by employing organic solvents having a refractive index intermittant to that of the matrix and polymer. The resulting repulsive van der Waals force then will effectively eliminate the hazards of adsorption.

Separation of Variables. A final comment should be made on the separation of variables in eq 34. For spherical solutes, this is trivial and a number of spherical solutes, proteins and viruses, thus provide a clearcut reference value for the maximal $\bar{x}$. This is achieved by a maximally charged solute of given size within one given column that is likely not maximally charged. Surprisingly, rod-shaped solutes representing the entire configuration range from stiff to somewhat coiled (TMV and DNA as well as intermediate filament oligomers studied previously[15]) exhibit similar $\bar{x}$ values as found for spheres of the same size R_{SEC}. If generally verified, this would mean that the rotational average of arbitrary shapes with "soft" boundaries corresponds to the rotational average of the core body plus its appropriate interfacial terms. Consequently, porous coils might be represented by hydrodynamically equivalent spheres upon which the charges are placed with far-reaching mathematical amenities in their physical description. Clearly one should next test the validity of separation of terms for arbitrary charge densities.

Alternate Theories. The magnitude of observed maximal $\bar{x}$ values and the Spherosil QMA study[40] (see above) may raise desire for altogether alternative interpretations. One is that the matrix is simply undergoing alterations with ionic strength. Certainly soft gels have been reported to swell, and the entire outlined analysis would then require correction terms—if not becoming entirely impractical. Swelling of the TSK PW matrix has been excluded experimentally by observing constant void volumes (Table II). A more peculiar facet is the internal surface structure of microparticulate beads formed by gradual condensation of nodules that are subsequently fused. The nodule density presumably decreases from their center to their surface related to fractal properties[154] and Heitz and Kern[155] have envisaged a brush-type surface formed by protruding polymer tails. The manufacture of TSK PW is proprietory but presumably belongs to this type of matrix, and it is unknown whether TSK PW has been cured by cross-linking protruding tails to the pore surface in a later production step. If such tails existed and expanded with decreasing ionic strength, effectively moving the pore wall, one should have observed changed elution of neutral V_{tot} markers like vitamin B_{12} (see Figure 4) as well as shifted elution for any uncharged molecule or polyelectrolytes at their pI. Furthermore, several investigated matrices may be a priori excluded to bear such flexible surfaces. Thus, mechanical constructs are no viable alternative to the proposed treatment in terms of interfacial energies.

Interpretation of Interfacial Separation Distances. R_{IF} mutually depends on the properties of both walls and is not the property of an individual isolated molecule. Operational splitting into additive contributions at the position of minimal interaction energy, following the notion of surface potentials (see insert of Figure 7), leads to the picture of a counterion cage,[2] but this may be deceiving even if duly generalized to local deviations of any kind from the bulk solvent properties. The energetically defined spacial contour of a body only originates from interaction with a sensor as is true for any criterium to define a spacial entity. It is a matter of chromatographic procedures and convenience to lump all variables into a solute-specific dimension R. Chromatography will provide ample variation to study interfacial phenomena, local surface curvature and size, charge and chemical nature, of both the solute and the matrix in addition to variations of the solvent properties. Having one component structurally fixed and the other at infinite dilution is a definite methodological advantage over fluidlike colloidal systems.

6. Biological Conclusions. The observation of interfacial interaction between a porous matrix and its contained solutes is of crucial importance for inverse chromatography. The latter has been applied to determine the diameters of membrane pore complexes. The complement protein assembly creates pores with a maximum ultrastructural diameter of 11 nm[156] and a functional permeability limit of 6–7 nm.[157] Thus, $R_{IF} \sim 2.5$ nm for $R_\eta \sim 3$ nm. Killer lymphocytes secernate a protein that forms cytolytic pores on their selected target cells, similar to the complement protein assembly, and thereby kill

them. The maximum pore diameter is 10 nm based on the permeability of small molecules in terms of their Stokes radii and 16 nm by electron microscopy.[158] This difference (i.e., $R_{IF} \simeq 3$ nm for $R_\eta \sim 5$ nm) is perfectly consistent with the present consideration of interfacial effects. It may correspond to the limit of hydration forces or equally to an appropriate $\bar{x} \simeq 4$.

At high concentration, TMV forms oriented gels whose interparticle spacing has been studied by X-ray diffraction as a function of osmotic stress. From this, one may extrapolate to the equilibrium distances that are reported to be equivalent to $\bar{x} = 12$,[159] comparable to the chromatographically determined numbers (Figure 6).

Another test is the solubility of proteins. Erythrocytes are packed with hemoglobin to the limits, viz. 280 mg/mL. Assuming a semiliquid arrangement, one may calculate (see Table I) a mean particle separation and find $R_{IF} \simeq 3$ nm for $R_\eta = 3.1$ nm. This again is within the general trend. The large variation of R_{IF} with particle size predicts peculiar properties for the solubility of mixtures of differently sized proteins or other particle emulsions. Thus, our results bear technological importance for the formulation of multicomponent colloidal systems.

The cytoskeleton of cells forms a network of interconnected fibrils similar to a chromatographic matrix. Details remain controversial, but judging from chromatographic theory,[128,160] the diffusion of dextran in the cytoplasm of HTC cells[161] seems best explained by a functional exclusion size of $R_S \sim 6$ nm superimposed onto a slow mobility that is coupled with the continuous rearrangement of the cytoskeleton. A proper account of the interfacial repulsion, which has been detailed in this paper, then leads to a pore diameter of 15–20 nm. Considering the additional osmotic pressure due to the high concentration of interdigitated soluble components, this matches the distance that interfacial repulsion imposes on highly charged large structural segments at physiological ionic strength. It suggests that retarded DLVO forces may be crucial determinants of cytoskeletal supramolecular organization. Dextrans were chosen for this assessment since proteins additionally seem to adsorb to the cytoplasmic matrix; previously reported binding constants (see ref 161), however, neglect purely hydrodynamic effects and are likely too high. Hydrodynamic evidence indicates that the cytoskeletal pore size in solution, which varies with cell type, is smaller than estimated from electron microscopy.[84] Thus, the microtrabecular lattice as visualized may be a preparative condensation artifact (see refs 162 and 163) even though a fine mesh work indeed seems to exist. The outlined paradigm now has to be filled with a systematic physical characterization of archetypical structural patterns. One is the abundance of brushlike tails protruding from larger cytoskeletal filaments in a variety of biochemical/genetic realizations. Work in this direction is progressing. One crucial implication of the present study is clear, however. If it were not for the huge size dependency of interfacial repulsion, small substrates, enzymes, and messengers could not pass freely through the cytoskeletal lattice, and life would not be possible as presently perceived.

Summary

This study investigated the static and dynamic properties of differently shaped solutes within porous networks. Primarily a chromatographic concern, the scope is not limited to SEC. A generalized theory of universal calibration is advanced that also accounts for interfacial effects between pore wall and solute surface in addition to the traditional concern of a proper rotational average for an arbitrary solute shape. The latter is referred to here as the equivalent chromatographic radius (R_{SEC}) and is at least similar if not identical with the hydrodynamic viscosity radius (R_η). Possible exceptions are DNA, which has been characterized in detail in the present study, and schizophyllan, where $R_G \gg R_{SEC} \geq R_\eta$, subject to further investigations. The other notable exception concerns protein–SDS complexes where apparently $R_\eta > R_S \geq R_{SEC}$, uncorrelated to persistence length, which is almost identical with DNA. Again this system demands further clarification. Xanthan, having a persistence length close to DNA and protein–SDS complexes, has been reported to elute according to R_η. Furthermore, the slightly more flexible NaPSS elutes according to R_η, but its structural counterpart heparin supposedly elutes earlier. The seemingly arbitrary elution properties of these systems are thus not correlated with their supposed physical structure, and no consistent theory to explain these deviations is currently available. Presumably the physicochemical definition of these systems first needs to be improved.

The chromatographic size of solutes is actually not defined by their hydrodynamic boundaries but by their interfacial interaction with the pore walls. This interfacial contribution (R_{IF}) to the total effective radius (R) has been studied in the special case of maximally charged polyelectrolytes. R_{IF} then is found to be a linear function of $I^{-1/2}$ within experimental errors, independent of net charge, and increases with increasing R_{SEC}. This increase is larger than can be explained by electrostatic interaction alone, and retarded van der Waals forces were found to contribute crucially. In fact, SEC promises general potential for characterizing surface forces. The interfacial properties investigated have a general bearing on the static stability of complex supramolecular and colloidal systems. Thus, the present data on large solutes bridge the gap between smaller solutes studied previously[2] and the colloidal dimensions of porous networks themselves. They demonstrate that porous networks established by their own interfacial forces are nonetheless permeable to smaller particles that are subject to the same principles, simply because the interfacial forces strongly depend on size, i.e., curvature of the surfaces.

Acknowledgment. The collaboration with Stefan Diekmann for preparing the DNA is gratefully acknowledged.

References and Notes

(1) Potschka, M. *Anal. Biochem.* **1987**, *162*, 47.
(2) Potschka, M. *J. Chromatogr.* **1988**, *441*, 239.
(3) Dubin, P. L.; Principi, J. M. *Macromolecules* **1989**, *22*, 1891.
(4) Verway, E. J. W.; Overbeek, J. T. J. *Theory of the Stability of Lyophobic Colloids*; Elsevier: Amsterdam, 1948.
(5) Potschka, M.; Koch, M. H. J.; Adams, M. L.; Schuster, T. M. *Biochemistry* **1988**, *27*, 8481.
(6) Diekmann, S.; Wang, J. C. *J. Mol. Biol.* **1985**, *186*, 1.
(7) Eigner, J.; Doty, P. *J. Mol. Biol.* **1965**, *12*, 549.
(8) Godfrey, J. E. *Biophys. Chem.* **1976**, *5*, 285.
(9) Godfrey, J. E.; Eisenberg, H. *Biophys. Chem.* **1976**, *5*, 301.
(10) Lansing, W.; Kraemer, E. *J. Am. Chem. Soc.* **1935**, *57*, 1369.
(11) Kovacic, R. T.; van Holde, K. E. *Biochemistry* **1977**, *16*, 1490.
(12) Prunell, A.; Bernardi, G. *J. Biol. Chem.* **1973**, *248*, 3433.
(13) Record, M. T.; Woodbury, C. P. *Biopolymers* **1975**, *14*, 393.
(14) Himmel, M. E.; Squire, P. G. *J. Chromatogr.* **1981**, *210*, 443.
(15) Potschka, M.; Nave, R.; Weber, K.; Geisler, N. *Eur. J. Biochem.* **1990**, *190*, 503.
(16) Ohshima, H.; Healy, T. W.; White, L. R. *J. Colloid Interface Sci.* **1982**, *90*, 17.
(17) Bell, G. M.; Levine, S.; Mc Cartney, L. N. *J. Colloid Interface Sci.* **1970**, *33*, 335.

(18) Prieve, D. C.; Hoysan, P. M. *J. Colloid Interface Sci.* **1978**, *64*, 201.
(19) Silebi, C. A.; Mc Hugh, A. J. *Am. Inst. Chem. Eng. J.* **1978**, *24*, 204.
(20) Malone, D. M.; Anderson, J. L. *Chem. Eng. Sci.* **1978**, *33*, 1429.
(21) Smith, F. G., III; Deen, W. M. *J. Colloid Interface Sci.* **1983**, *91*, 571.
(22) Brenner, S. L.; Parsegian, V. A. *Biophysical J.* **1974**, *14*, 327.
(23) Stigter, D. *J. Colloid Interface Sci.* **1975**, *53*, 296.
(24) Parsegian, V. A.; Rand, R. P.; Rau, D. C. In *Physics of Complex and Supermolecular Fluids*; Safran, S. A., Clark, N. A., Eds.; Wiley: New York, 1987; p 115.
(25) Evans, E. A.; Parsegian, V. A. *Proc. Natl. Acad. Sci. U.S.A.* **1986**, *83*, 7132.
(26) Millman, B. M.; Irving, T. C.; Nickel, B. G.; Loosley-Millman, M. E. *Biophys. J.* **1984**, *45*, 551.
(27) Nozaki, Y.; Schechter, N. M.; Reynolds, J. A.; Tanford, C. *Biochemistry* **1976**, *15*, 3884.
(28) Israelachvilli, J. N. *Intermolecular and Surface Forces*; Academic Press: London, 1985.
(29) Hamaker, H. C. *Physica* **1937**, *4*, 1058.
(30) Mahanty, J.; Ninham, B. W. *Dispersion Forces*; Academic Press: New York, 1976.
(31) Clayfield, E. J.; Lumb, E. C. *Disc. Faraday Soc.* **1966**, *42*, 285.
(32) Wiese, G. R.; Healy, T. W. *Trans. Faraday Soc.* **1970**, *66*, 490.
(33) Janča, J. *Adv. Chromatogr.* **1981**, *19*, 37.
(34) Audebert, R. *Polymer* **1979**, *20*, 1561.
(35) Coll, H.; Gilding, D. K. *J. Polym. Sci. A-2* **1970**, *8*, 89.
(36) Anger, H.; Berth, G. *Carbohydr. Polym.* **1985**, *5*, 241.
(37) Belenkii, B. G.; Vilenchik, L. Z.; Nesterov, V. V.; Kolegov, V. J.; Frenkel, S. Y. *J. Chromatogr.* **1975**, *109*, 233.
(38) Callec, G.; Anderson, A. W.; Tsao, G. T.; Rollings, J. E. *J. Polym. Sci. Polym. Chem. Ed.* **1984**, *22*, 287.
(39) Deckers, H. A.; Olieman, C.; Rombouts, F. M.; Pilnik, W. *Carbohydr. Polym.* **1986**, *6*, 361.
(40) Domard, A.; Rinaudo, M. *Polym. Commun.* **1984**, *25*, 55.
(41) Dubin, P. L.; Levy, I. J. *J. Chromatogr.* **1982**, *235*, 377.
(42) Dubin, P. L.; Tecklenburg, M. M. *Anal. Chem.* **1985**, *57*, 275.
(43) Fishman, M. L.; Damert, W. C.; Phillips, J. G.; Barford, R. A. *Carbohydr. Res.* **1987**, *160*, 215.
(44) Frigon, R. P.; Leypoldt, J. K.; Uyeji, S.; Henderson, L. W. *Anal. Chem.* **1983**, *55*, 1349.
(45) Guise, G. B.; Smith, G. C. *J. Chromatogr.* **1982**, *235*, 365.
(46) Hennink, W. E.; Van den Berg, J. W. A.; Feijen, J. *Thrombosis Res.* **1987**, *45*, 463.
(47) Horiike, K.; Tojo, H.; Yamano, T.; Nozaki, M. *J. Biochem.* **1983**, *93*, 99.
(48) Imamura, T.; Konishi, K.; Yokoyama, M.; Konishi, K. *J. Liq. Chromatogr.* **1981**, *4*, 613.
(49) Kato, T.; Tokuya, T.; Takahashi, A. *J. Chromatogr.* **1983**, *256*, 61.
(50) Kuga, S. *J. Chromatogr.* **1981**, *206*, 449.
(51) Kuge, T.; Kobayashi, K.; Tanahashi, H.; Igushi, T.; Kitamura, S. *Agric. Biol. Chem.* **1984**, *48*, 2375.
(52) Lambert, F.; Milas, M.; Rinaudo, M. *Polym. Bull.* **1982**, *7*, 185.
(53) Leloup, V. M.; Colonna, P.; Ring, S. G. *Macromolecules* **1990**, *23*, 862.
(54) Le Maire, M.; Viel, A.; Møller, J. V. *Anal. Biochem.* **1989**, *177*, 50.
(55) Mori, S. *Anal. Chem.* **1989**, *61*, 530.
(56) Pérez-Payá, E.; Braco, L.; Campos, A.; Soria, V.; Abad, C. *J. Chromatogr.* **1989**, *461*, 229.
(57) Rochas, C.; Domard, A.; Rinaudo, M. *Eur. Polym. J.* **1980**, *16*, 135.
(58) Spatorico, A. L.; Beyer, G. L. *J. Appl. Polym. Sci.* **1975**, *19*, 2933.
(59) Squire, P. G. *J. Chromatogr.* **1981**, *210*, 433.
(60) Styring, M. G.; Price, C.; Booth, C. *J. Chromatogr.* **1985**, *319*, 115.
(61) Talley, C. P.; Bowman, L. M. *Anal. Chem.* **1979**, *51*, 2239.
(62) Dubin, P. L. *Adv. Chromatogr.*, in press.
(63) Kato, Y.; Hashimoto, T. *J. Chromatogr.* **1982**, *235*, 539.
(64) Senak, L.; Wu, C. S.; Malawer, E. G. *J. Liq. Chromatogr.* **1987**, *10*, 1127.
(65) Engelhardt, H.; Mathes, D. *J. Chromatogr.* **1979**, *185*, 305.
(66) Bailey, F. E.; Koleske, J. V. In *Nonionic Surfactants*; Schick, M. J., Ed.; Dekker: New York, 1967; p 794.
(67) Kraus, S.; Rogers, L. B. *J. Chromatogr.* **1983**, *257*, 237.
(68) Rinaudo, M. Personal communication.
(69) Tinland, B.; Rinaudo, M. *Macromolecules* **1989**, *22*, 1863.
(70) Boháček, J.; Blažiček, G. *J. Polym. Sci. Polym. Symp.* **1980**, *68*, 121.
(71) Himmel, M. E.; Perna, P. J.; Mc Donell, M. W. *J. Chromatogr.* **1982**, *240*, 155.
(72) Chatterjee, B.; Koteswara Rao, G. R. *Indian J. Biochem. Biophys.* **1984**, *21*, 378.
(73) Edwardson, P. A. D.; Atkinson, T.; Lowe, C. R.; Small, D. A. P. *Anal. Biochem.* **1986**, *152*, 215.
(74) Gómez-Márquez, J.; Freire, M.; Segade, F. *Gene* **1987**, *54*, 255.
(75) Micard, D.; Sobrier, M. L.; Couderc, J. L.; Dastugue, B. *Anal. Biochem.* **1985**, *148*, 121.
(76) Moreau, N.; Tabary, X.; Le Goffic, F. *Anal. Biochem.* **1987**, *166*, 188.
(77) Norgand, M. V. *Anal. Biochem.* **1981**, *113*, 34.
(78) Raymond, G.; Bryant, P. K.; Nelson, A.; Johnson, J. D. *Anal. Biochem.* **1988**, *173*, 125.
(79) Whisenant, E. C.; Rasheed, B. K. A.; Bhatnagar, Y. M. *Nucl. Acid Res.* **1988**, *16*, 5202.
(80) Yoshinaga, K.; Suzuki, Y. *Agric. Biol. Chem.* **1983**, *47*, 919.
(81) Andersson, T.; Carlsson, M.; Hagel, L.; Pernemalm, P. A.; Janson, J. C. *J. Chromatogr.* **1985**, *326*, 33.
(82) Boyes, B. E.; Walker, D. G.; Mc Geer, P. L. *Anal. Biochem.* **1988**, *170*, 127.
(83) Dornburg, R.; Földi, P.; Hofschneider, P. H. *J. Chromatogr.* **1984**, *296*, 379.
(84) Dornburg, R.; Kruppa, J.; Földi, P. *LC Mag.* **1986**, *4*, 22.
(85) Ellegren, H.; Låås, T. *J. Chromatogr.* **1989**, *467*, 217.
(86) Kato, Y.; Sasaki, M.; Hashimoto, T.; Murotsu, T.; Fukushige, S.; Matsubara, K. *J. Chromatogr.* **1983**, *266*, 341.
(87) Kato, Y.; Sasaki, M.; Hashimoto, T.; Murotsu, T.; Fukushige, S.; Matsubara, K. *J. Biochem.* **1984**, *95*, 83.
(88) Kato, Y.; Yamasaki, Y.; Hashimoto, T.; Murotsu, T.; Fukushige, S.; Matsubara, K. *J. Chromatogr.* **1985**, *320*, 440.
(89) Makino, K.; Hatano, H. In *Aqueous size exclusion chromatography*; Dubin, P. L., Ed.; Elsevier: Amsterdam, 1988; p 235.
(90) Schmitter, J. M.; Mechulam, Y.; Fayat, G.; Anselme, M. *J. Chromatogr.* **1986**, *378*, 462.
(91) Mc Pherson, D. D.; Pezzuto, J. M. *J. Chromatogr.* **1983**, *281*, 348.
(92) Persson, H.; Perricaudet, M.; Tolun, A.; Philipson, L.; Pettersson, U. *J. Biol. Chem.* **1979**, *254*, 7999.
(93) Fukumoto, T.; Nishimura, T.; Nagasawa, T.; Kitajima, K.; Iwamura, T. *Anal. Biochem.* **1988**, *170*, 463.
(94) Odijk, T. *Biopolymers* **1979**, *18*, 3111.
(95) Smidsrød, O.; Haug, A. *Biopolymers* **1971**, *10*, 1213.
(96) Suzuki, H.; Sasaki, T. *Bull. Chem. Soc. Jpn.* **1971**, *44*, 2630.
(97) Birdi, K. S. In *Aqueous size exclusion chromatography*; Dubin, P. L., Ed.; Elsevier: Amsterdam, 1988; p 399.
(98) Tanford, C.; Nozaki, Y.; Rohde, M. F. *J. Phys. Chem.* **1977**, *81*, 1555.
(99) Robson, R. J.; Dennis, E. A. *Biochem. Biophys. Acta* **1978**, *508*, 513.
(100) Dubin, P. L.; Principi, J. M.; Smith, B. A.; Fallon, M. A. *J. Colloid Interface Sci.* **1989**, *127*, 558.
(101) Ollivon, M.; Walter, A.; Blumenthal, R. *Anal. Biochem.* **1986**, *152*, 262.
(102) Okazaki, M.; Hara, I. In *Aqueous size exclusion chromatography*; Dubin, P. L., Ed.; Elsevier: Amsterdam, 1988; p 297.
(103) Lundahl, P.; Greijer, E.; Sandberg, M.; Cardell, S.; Eiksson, K. O. *Biochem. Biophys. Acta* **1986**, *873*, 20.
(104) Wright, A. K.; Thompson, M. R.; Miller, R. L. *Biochemistry* **1975**, *14*, 3224.
(105) Fish, W. W.; Reynolds, J. A.; Tanford, C. *J. Biol. Chem.* **1970**, *245*, 5166.
(106) Tanford, C.; Nozaki, Y.; Reynolds, J. A.; Makino, S. *Biochemistry* **1974**, *13*, 2369.
(107) Waldmann-Meyer, H. *J. Chromatogr.* **1985**, *350*, 1.
(108) Collins, R. C.; Haller, W. *Anal. Biochem.* **1973**, *54*, 47.
(109) Montelaro, R. C.; West, M.; Issel, C. J. *Anal. Biochem.* **1981**, *114*, 398.
(110) Takagi, T.; Takeda, K.; Okuno, T. *J. Chromatogr.* **1981**, *208*, 201.
(111) Imamura, T.; Konishi, K.; Yokoyama, M.; Konishi, K. *J. Biochem.* **1979**, *86*, 639.
(112) Pitt-Rivers, R.; Ambesi Impiombato, F. S. *Biochem. J.* **1968**, *109*, 825.
(113) Makino, S.; Niki, R. *Biochem. Biophys. Acta* **1977**, *495*, 99.
(114) Robinson, N. C.; Tanford, C. *Biochemistry* **1975**, *14*, 369.
(115) Reynolds, J. A.; Tanford, C. *J. Biol. Chem.* **1970**, *245*, 5161.
(116) Kato, Y.; Komiya, K.; Sasaki, H.; Hashimoto, T. *J. Chromatogr.* **1980**, *193*, 29.
(117) Frenkel, M. J.; Blagrove, R. J. *J. Chromatogr.* **1974**, *111*, 397.
(118) Freytag, J. W.; Noelken, M. E.; Hudson, B. G. *Biochemistry* **1979**, *18*, 4761.
(119) Leach, B. S.; Collawn, J. F.; Fish, W. W. *Biochemistry* **1980**, *19*, 5734.
(120) Eriksson, K. O. *J. Biochem. Biophys. Meth.* **1985**, *11*, 145.
(121) Miyake, J.; Ochiai-Yanagi, S.; Kasumi, T.; Takagi, T. *J. Biochem.* **1978**, *83*, 1679.

(122) Shirahama, K.; Tsujii, K.; Takagi, T. *J. Biochem.* **1974**, *75*, 309.
(123) Le Maire, M.; Rivas, E.; Møller, J. V. *Anal. Biochem.* **1980**, *106*, 12.
(124) Le Maire, M.; Aggerbock, L. P.; Monteilhet, C.; Anderson, J. P.; Møller, J. V. *Anal. Biochem.* **1986**, *154*, 525.
(125) Styring, M. G.; Davison, C. J.; Price, C.; Booth, C. *J. Chem. Soc. Faraday Trans. 1* **1984**, *80*, 3051.
(126) De Haen, C. *Anal. Biochem.* **1987**, *166*, 235.
(127) Waldmann-Meyer, H. *J. Chromatogr.* **1987**, *410*, 233.
(128) Potschka, M. Manuscript in preparation.
(129) Mazsaroff, I.; Thevenon, G.; Yang, Y. B.; Fulton, S.; Várady, L.; Regnier, F.; Afeyan, N. Presented at the 9th Int. Symp. on HPLC of Proteins, Peptides and Polynucleotides, Philadelphia, 1989.
(130) Haller, W. *Macromolecules* **1977**, *10*, 83.
(131) Basedow, A. M.; Ebert, K. H.; Ederer, H. J.; Posshag, E. *J. Chromatogr.* **1980**, *192*, 259.
(132) Hagel, L. In *Aqueous size exclusion chromatography*; Dubin, P. L., Ed.; Elsevier: Amsterdam, 1988; p 119.
(133) Haller, W. *Nature* **1965**, *206*, 693.
(134) Tanford, C. *Physical Chemistry of Macromolecules*; Wiley: New York, 1961; p 409.
(135) Booth, C.; Forget, J. L.; Georgii, I.; Li, W. S.; Price, C. *Eur. Polym. J.* **1980**, *16*, 255.
(136) Crone, H. D. *J. Chromatogr.* **1974**, *92*, 127.
(137) Rinaudo, M.; Desbrieres, J. *Eur. Polym. J.* **1980**, *16*, 849.
(138) Small, H. *Adv. Chromatogr.* **1977**, *15*, 113.
(139) Styring, M. G.; Honing, J. A. J.; Hamielec, A. E. *J. Liq. Chromatogr.* **1986**, *9*, 3505.
(140) Dubin, P. L.; Speck, C. M.; Kaplan, J. I. *Anal. Chem.* **1988**, *60*, 895.
(141) Jönsson, B.; Wennerström, H. *J. Chem. Soc. Faraday Trans. 2* **1983**, *79*, 13.
(142) Kjellander, R. *J. Chem. Soc. Faraday Trans. 2* **1984**, *80*, 1323.
(143) Barrall, E. M.; Cain, J. H. *J. Polym. Sci. C* **1968**, *21*, 253.
(144) Kirkland, J. J. *J. Chromatogr.* **1976**, *125*, 231.
(145) van Kreveld, M. E.; van den Hoed, N. *J. Chromatogr.* **1973**, *83*, 111.
(146) Ungar, K. K.; Gimpel, M. G. *J. Chromatogr.* **1979**, *180*, 93.
(147) Millar, J. R.; Smith, D. G.; Marr, W. E.; Kressman, T. R. E. *J. Chem. Soc.* **1963**, 183.
(148) Mikeš, O.; Štrop, P.; Čoupek, *J. J. Chromatogr.* **1978**, *153*, 23.
(149) Kato, Y.; Kitamura, T.; Hashimoto, T. *J. Chromatogr.* **1985**, *333*, 93.
(150) Hagel, L.; Lundström, K.; Andersson, T.; Lindblom, H. *J. Chromatogr.* **1989**, *476*, 329.
(151) Amsterdam, A.; Er-El, Z.; Shaltiel, S. *Arch. Biochem. Biophys.* **1975**, *171*, 673.
(152) Spencer, M. *J. Chromatogr.* **1982**, *238*, 317.
(153) Attwood, T. K.; Nelmes, B. J.; Sellen, D. B. *Biopolymers* **1988**, *27*, 201.
(154) Brickmann, J. In *Ordnung und Chaos in der unbelebten und belebten Natur*; Gerok, W., Haken, H., zur Hausen, H., Nachtigall, W., Roesky, H. W., Nöth, H., Gibian, H., Eds.; Wissenschaftliche Verlagsgesellschaft: Stuttgart, 1989; p 229.
(155) Heitz, W.; Kern, W. *Angew. Makromol. Chem.* **1967**, *1*, 150.
(156) Müller-Eberhard, H. J. *Annu. Rev. Biochem.* **1988**, *57*, 321.
(157) Mayer, M. M. In *Mechanisms of cell-mediated cytotoxicity*; Clark, W. R., Goldstein, P., Eds.; Plenum: New York, 1982; p 193.
(158) Young, J. D-E.; Cohn, Z. A. *Sci. Am.* **1988**, *258* (Jan), 28.
(159) Millman, B. M.; Nickel, B. G. *Biophys. J.* **1980**, *32*, 49.
(160) Weber, S. G.; Carr, P. W. *Chem. Anal.* **1989**, *98*, 1.
(161) Peters, R. *Biochem. Biophys. Acta* **1986**, *864*, 305.
(162) Kondo, H. *J. Ultrastructure Res.* **1984**, *87*, 124.
(163) Ris, H. *J. Cell Biology* **1985**, *100*, 1474.